Addis Ababa University (AAU)

Addis Ababa Institute of Technology (AAiT)

School of Mechanical and Industrial Engineering

Wheel Rail Interaction Modeling on Rail Vehicle System Lateral Dynamics

A Thesis submitted to the School of Graduate studies of Addis Ababa institute of Technology in Partial Fulfillment of the Requirement for the Degree of Master of Science in Railway Engineering

(Rolling Stock)

By

Birhan Abebaw

Under supervision of

Dr. In. Zewdu Abdi

Ato Tollosa Deberie

September 2014

Addis Ababa University (AAiT)

Addis Ababa Institute of Technology (AAiT)
School of Mechanical & Industrial Engineering
Railway Engineering Stream

Wheel-Rail Interaction Modeling on Rail Vehicle system Lateral Dynamics.

By

Birhan Abebaw

Approved by Board of Examiners

---------- _____
Chairman of Railway center

Doc. In. Zewdu Abdi
---------- _____
Advisor

Ato Tollosa Deberie
---------- _____
Co-Advisor

---------- _____
Internal Examiner

---------- _____
External Examiner

Declaration

I hereby declare that the work which is being presented in this thesis entitled "***Wheel-Rail Interaction Modeling on Rail Vehicle system Lateral Dynamics***." is original work of my own, has not been presented for a degree of any other university and all the resource materials used for this thesis have been duly acknowledged.

_____ _____

Birhan Abebaw Date

This is to certify that the above declaration made by the candidate is correct to the best of my knowledge.

_____ _____

Doc. In. Zewdu Abdi (Advisor) Date

_____ _____

Ato Tollosa Deberie (Co-advisor) Date

Acknowledgment

I would like to express my sincere gratitude to my advisors Dr. In. Zewdu Abdi and Ato Tollesa Deberie for giving me the opportunity to work on this project and for their guidance and encouragement without which this work could have not been completed. They have been a constant source of inspiration throughout my study period. I am also thanks to Ato Fikadu for his kind help on different occasions.

Last but not least, I would like to thank my family and friends who were always besides me and played a great role in completion of my work.

Abstract

The long history of railway engineering provides many practical examples of dynamic problems which are unique to railway vehicles. One of the railway vehicle's dynamic problems is the lateral dynamic which is mainly arising from wheel rail contact condition. In the early time, to analyze and formulate such kinds of railway vehicle dynamics scientists had been using different experimental methods such as roller rigs and roller coasters. Even though such experimental methods are most efficient and error free, they are very costly and need some time. But now a day there are different computer packages used to study and simulate the dynamic behavior of a railway vehicle (ADAMS/RAIL, SIMPAKC and Vampire). These computational packages are very efficient in both cost and time but they are not more flexible and require in-depth knowledge to run them. So this paper tried to make the computational tool more flexible and easy to use with basic computer knowledge

In the work presented, mathematical model and computational tool used for the dynamic simulation of railway vehicle wheelset systems was developed using multibody systems formulations. The model based on the multibody techniques developed by Shabana. With respect to other exciting methodologies the proposed one make use of a combined frame of references that permit the use of independent coordinates, without the possibility to have singularity configurations depending on the rotation sequence. Lagrangian Equation of motions such as virtual work and kinetic and potential energy are used to develop the equation of motion. Finally a MATLAB program is developed to analyze the dynamic behavior of the wheelset at different velocities on a straight track. The program was designed to considering the flexibility of different configuration of railway vehicles. The model used was applied to make a simulation for single wheelset.

The analysis were made for different velocities, lower than the critical in which the vehicle responded in stable form, and higher than the critical at which the instability of the vehicle was studied. The obtained results of the dynamic response for a defined track composed of tangent segment is analyzed and compared with one published paper.

Table of Contents

List of Figures

Abbreviations

MBC	Multibody system
CM	Centre of mass
K.E	Kinetic Energy
DAE	Differential Algebraic Equation
ODE	Ordinary Differential Equation

List of Symbols

Over script	
$\bar{a}$	Vector represented in Track frame of reference
$\bar{\bar{a}}$	Vector represented in Solid frame of reference
$\dot{a}$	First time derivative of vector a
$\ddot{a}$	Second time derivative of vector a
$\tilde{a}$	Skew-symmetric matrix

Down script	
$\underline{a}$	Vector represented in Intermediate reference frame

Superscript	
a^T	Transpose of vector
$\mathbf{A}^{\mathbf{T}}$	Transpose of matrix

Subscript	
a_r	Quantity referred to the rail
a_w	Quantity referred to the wheel
a_c	Quantity referred to the contact
a_{CM}	Quantity referred to center

Latin Symbols	
a, b	Longitudinal and transversal semi axis of the contact ellipse
A, B	Geometrical functions related to the principle and transversal radii of the curvature of the wheel and the rail

A	Transformation matrix from track frame to fixed frame
B	Transformation matrix from solid frame to track frame
$\mathbf{B}_{zx,}$	Transformation matrix from intermediate frame to track frame
$\boldsymbol{C_{11}}, \boldsymbol{C_{22}}, \boldsymbol{C_{23}}, \boldsymbol{C_{33}}$	Creepage and spin coefficients from Kalker's theory
$\boldsymbol{q}, \dot{\boldsymbol{q}}, \ddot{\boldsymbol{q}}$	Vectors of generalized coordinate, velocities and accelerations
$\boldsymbol{Q}$	Generalized force vector
E	Young's modulus
G	Track gauge
G	The combined shear modulus of rigidity of the rail and wheel material
K	Geometry parameter
I	Identity matrix
$\boldsymbol{J}$	Inertia matrix
R	Radius of curvature
XYZ	Global reference frame
$X_T Y_T Z_T$	Track reference frame
$X_S Y_S Z_S$	Solid reference frame
$\underline{X}\ \underline{Y}\ \underline{Z}$	Intermediate reference frame
M	System mass matrix
M_C	Moment of the contact patch
m	Rigid body mass
n	Principal unit normal vector
l	Principal unit longitudinal vector
t	Principal unit lateral vector

Greek Symbols	
$\boldsymbol{\delta}$	Indentation (or penetration) during contact
$\boldsymbol{\gamma}$	Conicity of the wheel profile
$\boldsymbol{\omega}$	Solid angular velocity
$\boldsymbol{\tau}$	Track angular velocity
κ	Curvature
$\boldsymbol{\xi_x}$	Longitudinal Creepage
$\boldsymbol{\xi_y}$	Lateral Creepage
$\boldsymbol{\xi_{sp}}$	Spin Creepage
$\boldsymbol{\phi}$	Cant angle
θ	Pitch angle
$\boldsymbol{\psi}$	Yaw angle

1. Chapter One

1.1 Background of the study

The railway vehicle running along a track is one of the most complex dynamic systems in engineering. It has many degrees of freedom, the interaction between wheel and rail involves both complex geometry of wheel tread and rail head and non-conservative force generated by relative motion in the contact area, and there are many nonlinearities.

[31] In the analysis of the running behavior of the vehicle it is not sufficient to consider only the vehicle; but also the track must be taken into account. The problem to be solved is to determine the effect of the interaction between the running gear and the track, and both elements need to be considered when studying the performance.

The dynamics of railway vehicle represent a balance between the forces acting between the wheel and the rail, the inertia force and the forces exerted by the suspension and articulation.

One objective of the study of the dynamics of railway vehicle is the development of sufficiently detailed and validated mathematical models that permits the simulation of the actual motion, on a specified stretch of line, so that the performance of a specified design can be analyzed or a particular incident recreated. A second objective of a study of a railway vehicle dynamics is to develop analytical or numerical models describing the mechanism of various phenomena by the simple model possible.

[31] In recent decades there has been the growing interest in new railway vehicle design and consequently a desire for a better understanding of the dynamic behavior of a railway vehicle. Especially the development of high speed trains has led to studies of railway vehicle dynamics throughout the world. Among other things, the studies have dealt with the mathematical modeling of the railway vehicle and have resulted in the development of computer programs for simulation of the dynamic of railway vehicle wheelset. As examples we can mention VAMPIRE from BR Research in Derby, VOCODYM from INERTS in Paris, MEDYNA from DLR in Munich and SIDIVE from CAF in Spain. Also in Denmark, where Hans True has been engendered. This has led for instance to a PhD thesis by Jens Christian Jensen [Jensen,1995] as well as the present thesis.

The main application of this paper is to define the running behavior of the vehicle. When designing and operating a railway vehicle some questions arise:

- ✓ When is the vehicle running stably?
- ✓ when is the vehicle running unstably?

- ✓ How do the vehicle and the track interact, and which parameters influence the stability and the dynamics?

All these questions will be answered by this work.

1.1.1 The Railway wheelset

[32] The basic unit of a railway vehicle is the wheelset, Figure 1.1. The conventional wheelset of today has the following features: it consists of two wheels fixed on a common axle, so that each wheel rotates with a common angular velocity and a constant distance between the two wheels is maintained. Flanges are provided on the inside edge of the treads and the flange-way clearance allows, typically, ± 7−10 mm of lateral displacement to occur before flange contact. Whilst many wheelsets commence life with purely coned treads, typically coned at 1/20 or 1/40, these treads wear rapidly in service, so that the treads come to possess curvature in the transverse direction. Similarly, rails also possess curvature in the transverse direction.

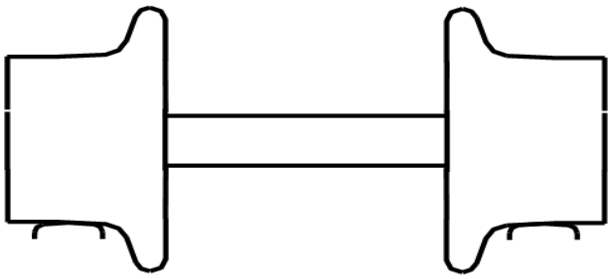

Figure 1-1 Railway wheelset

All these features contribute to the behavior of the railway vehicle as a dynamic system, and it is important to consider their purpose.

The conventional railway wheelset has a long history and seems to have evolved by a process of trial and error. Naturally, in the pioneering days of the early railways most attention was concentrated on reducing rolling resistance so that the useful load that could be hauled by horses could be multiplied. Another major problem was the lack of strength and resistance to wear of the materials then available. Moreover, the level of adhesion between rolling wheel and the track was unknown. As a result, many possibilities were tried. An obvious step was to fit wheels with cylindrical treads. However, if the wheels are fixed on the axle and the treads are intended to be cylindrical very slight errors in parallelism would induce large lateral displacements which would be limited by flange contact. There is no guidance until flange contact and thus a wheelset with cylindrical treads tends to run in continuous flange contact. The position of the flange, either inside or outside the rails, was controversial well into the nineteenth century. Nor was there agreement as to whether the wheels should be rigidly fixed to an axle or free to revolve on the axle, though the usual practice

seemed to be that wheels were fixed to the axle. The play allowed between wheel flange and rail was initially minimal. In the early 1830s the flange-way clearance was opened up with the objective of reducing the lateral forces between wheel and rail.

A further important point is that the geometry of the wheel and rail as it has evolved is particularly favorable for the method of switching which involves a minimum of moving parts and only small gaps in the running surfaces of the rails.

1.1.2 Creep

Pure rolling rarely takes place, and wheels and rails are not rigid. The normal load between wheel and rail causes local elastic deformation and an area of contact, the contact patch, is formed. In the case where the surfaces of the wheels and rails are smooth and have constant curvature in the vicinity of the contact patch, Hertz [7] showed that the contact patch was elliptical in shape, and the distribution of normal pressure between wheel and rail over the contact patch is semi-ellipsoidal.

If a longitudinal force is applied to the wheel, so that it is broken, a deviation from the pure rolling motion occurs. The deviation in relative velocity divided by the forward speed of the wheel is referred to as the longitudinal creepage. Similarly, lateral creepage is defined as the (incremental) relative lateral velocity divided by the forward speed. In addition, relative angular motion between wheel and rail about the normal to the contact patch is referred to as spin. If the longitudinal creepage is small, it is accommodated by elastic strains in the vicinity of the contact patch. As the wheel rotates, unstrained material enters the contact patch at its leading edge. As the material moves through the contact patch, the relative velocity between the wheel and rail equals the rate of change of strain so that the surfaces are locked together. The magnitude of the resulting longitudinal tangential stress increases linearly with distance from the leading edge. Similarly, lateral creepage gives rise to lateral tangential stresses. Both longitudinal and lateral creepage therefore generate forces which are directly proportional to the corresponding creepage. When there is spin, the pattern of elastic strain is more complicated.

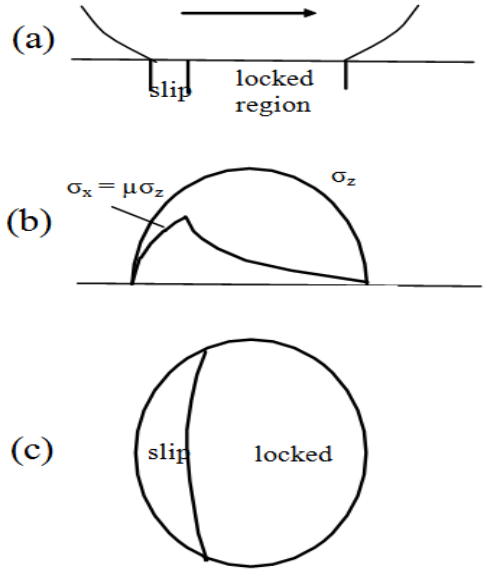

Figure 1-2 The contact patch between wheel and rail

[Source-32]

a) *Elevation showing locked region of adhesion at leading edge and region of slip at trailing edge*
b) *Normal pressure σ_z and tangential traction applied by wheel to rail σ_x*
c) *Contact patch in plain view.*

In this case, as the material moves through the contact region the relative velocity between wheel and rail is directly proportional to the distance from the center of the contact region and therefore the strain field becomes curved. As a consequence, a lateral force is generated (the couple about the common normal is small and may be safely neglected)

1.1.3 Degree of freedom

[31] In railway dynamics the bodies are often assumed to be rigid. This means that the elasticity of the body and shifting of the weight are neglected. A rigid body, which can move freely, has six degree of freedom. These degrees of freedoms are illustrated coordinate system in figure below

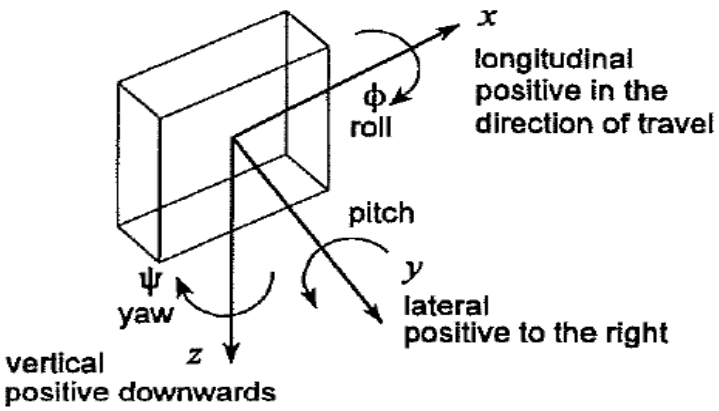

Figure 1-3 The degree of freedom for rigid body

[Source – 31]

There are three degrees of freedom (longitudinal *x*, lateral *y*, and vertical *z*) to define the position of the center of gravity from an initial system and three degrees of freedom (roll Φ, pitch and yaw Ψ) to define the rotation of the body about the longitudinal, lateral and vertical axes.

Consequently the mathematical system consisting of *N* rigid bodies can generally be described by equation of motion consisting of *6N* second order differential equations. Constrains of rigid bodies will reduce the independent degrees of freedom. We must decide, which degrees of freedom it important to include the model.

1.1.4 Coordinate system and transformation matrix

We use Newton's method to set up the equations of motion for the vehicle. The equations of motion are derived by projecting forces and rotations on to the three axes in an inertial coordinate system. To transfer forces and moments to an inertial system we have to define the various coordinate system and the necessary transformation matrices.

1.1.5 The equation of motion

In principle there are two philosophies in simulating the contact between wheel and rail in the railway vehicle. One can treat the wheel-rail contact as kinematic constraints, or one can treat the wheel-rail contact as locally elastic allowing a penetration of the wheel into the rail. Using the first method the equations of motion will consist of differential equation coupled with a set of algebraic equations determining the kinematic constrains of the normal force. Using the elastic approach we obtain instead of a set of ordinary differential equations.

1.1.6 Kinematics and Dynamics of Multibody System

Recently the derivations of equation of motion for the multibody system (MBS) were presented in a variety of forms by Nikravesh (1988), Shabana (1989), Huston (1990), Garcia de Jalon and Bayo (1994). For the rigid MBS, some technique allow us to generate the equation of motion in terms of a large set of dependent coordinates in the form of large set of mixed differential algebraic equation. Other techniques yield the equation of motion as a minimal set of ordinary differential equations. Many others in between approaches provide us with various alternatives.

1.2 Statement of the problem

In a railway vehicle system one of the main problems is its dynamic complexity problem which causes at least discomfort to the passengers and, at worst, the risk of derailment. From which one is lateral dynamics problem caused by wheel-rail contact. Now a day there are different excellent computer packages available, which provides sufficient detailed and validated mathematical models that can be used with confidence in engineering design and development. But most of them are not flexible and complex to use. Therefore, in the present paper the mathematical modeling and developed computational tool used to analyze the lateral dynamic behavior of wheelset are required to be more flexible and easy to use.

1.3 Thesis Organization

This paper is organized in to 7 chapters. In the first chapter, the introduction, method of the study, objective and overview of the thesis are discussed. In chapter two, literature review is given detailing information about the research. In chapter 3, detail discussions are given about reference frame and transformation of reference frame from one reference frame to another reference frame. In chapter four, track characterization, track geometry and cant angle definition are discussed and also mathematical models of track model is developed. In chapter five, multibody system of a wheelset is discussed, equation of motion of a wheelset is developed using its kinematic and dynamic analysis. In chapter 6, computational tool is developed using MATLAB environment and case study and obtained results are discussed. In the last chapter, conclusion and future development are discussed.

1.4 Significance of the study

Now a day our country, Ethiopia is implementing different projects of railway transportation and now we are not familiar enough with big computational tools developed on this area and some design analysis may not need such big tool. So this paper provides a more simple, flexible and easy to use mathematical model and computational tools developed on MATLAB environment. The computational tool is

used to analyze the lateral dynamic behavior of wheelset, arise from the wheel-rail contact, at different wheelset velocities and other parameters.

1.5 Objective of the study

1.5.1 General Objective

The general objective of this study is to assess factors that affect the dynamic behavior of a railway system vehicles' wheelset and develop a general mathematical equation of the dynamic system which consider all factors.

1.5.2 Specific Objective

- Developing mathematical model which consider all parameters affecting dynamic system (lateral dynamic system) of the vehicle's wheelset
- Generating computational tool in MATLAB environment.

1.6 Methodology of the Study

In order to achieve the objectives of this study the methodology used in this paper are listed below.

1.6.1 Literature Survey

To be familiar with the concept of multibody dynamic system and railway vehicles' wheelset dynamics different literature reviews were carried out. Articles and journals were also reviewed to reinforce this study.

1.6.2 Data Collection

Review of available data from the published journals, MSc papers and books were done for the comparison of the result of this paper.

1.7 Scope and Limitation of the Study

1.7.1 Scope of the study

The study is mainly focused on the modeling of the mathematical equation of the dynamic system of railway vehicle using multibody system and developing computational tools on MATLAB environment for the analysis of wheelset dynamic behavior at different lateral misalignment and forward velocity.

1.7.2 Limitation of the Study

The study is limited to the lateral dynamic behavior of the wheelset system of the vehicle and not the body of the vehicle. MATLAB program is developed for only the

straight line track and not for the transition or curved track. Track flexibility, track switches, track irregularities, vertical dynamics and flange or two point contacts are not considered in this paper.

The result of this thesis was compared with one published paper [33]. Due to lack of other software packed such as vampire and ADAMS, the result was not compared to these worldwide known software package results.

2 Chapter Two

2.1 Literature Review

Simulation of the dynamic behavior of railway vehicles is a complex topic in the railway dynamic field. Modern general-purpose softwares for the simulation of railway vehicle systems have included features that enable efficient dynamic analysis of the railway vehicles and vehicle-track interaction [4, 20, 30]. The dynamic behavior of railway vehicles relates to the motion or vibration of all the parts of the vehicle and is influenced by the vehicle design, particularly the suspension and the track on which the vehicle run. Due to this issue several models of simulation schemes were developed in which all the factors affecting the dynamics of a railway vehicle were studied, such as the model developed by S. Iwinicki and A. H. Wickens [10], in which a MATLAB computer program was developed in order to validate the results obtained by experimental measurements from a 1/5 scale roller rig used to evaluate the design change of the vehicle suspension system in Manchester University. The model used in the simulation and implemented in the MATLAB code was, a four-axel vehicle with a body and two bogies has been used. Each bogie has a frame including two wheelsets. All the bogies and the wheelsets are assumed to be rigid bodies connected by massless suspension elements. The instability in 1/5 roller rig has clearly been detected by the linear MATLAB program used and the model has provide more thorough re-examination of the effects of the errors due to the scaling and finite radius of the roller used, and usefulness of a roller rig analysis of railway behavior. During the last decades, the techniques using multibody approaches have evolved from manual graphics art to a highly specialized research field where the kinematics and dynamics of general mechanical systems are analyzed [20, 25, 29]. More efficient and reliable computer codes was developed to allow the formulation and the analysis of the dynamic behavior of a railway systems and solving the equations of motion of mechanical systems included with increasing the degree of complexity. Multibody computational methods can be used to simulate the dynamic effects of a vehicle components and the track, and the use of multibody algorithms which allow for the analysis of the nonlinear models, linearization schemes currently employed in railroad vehicle-track can be evaluated [26].

J. Pombo and J. Ambrósio [20, 23] has developed and implemented a computational tool suitable to study the dynamic behavior of rail guided vehicles in realistic operation conditions, an efficient multibody methodology was suggested and its computational implementation was discussed. The methodology proposed can be summarized in several points: the description of a three dimensional track model used for a roller coaster application [22, 23] and railway vehicle, obtaining realistic track conditions by definition and implementation of the track irregularities; development of a new methodology [21, 24] for the accurate prediction of the location of the contact points between the wheel and the rail surfaces; implementation of

several creep force models in order to compute all the tangential forces at the contact patch defined in the wheel-rail interaction area; finally validation of the multibody code presented in this work with modeling of a railway vehicle used by Lisbon metro company, and its performance was studied in real operation conditions and in different operation scenarios. The numerical results obtained from the computational tool proposed and the results obtained from ADAMS/RAIL Computer package used to study and simulate the performance of two railway vehicles in real operation conditions, was compared with experimental tests made on the railway vehicles to validate the obtained results.

Shabana et al. [28] presented a nonlinear finite element formulation for modeling the rail structural flexibility in multibody railroad vehicle systems, it was considered to use two types of interpolations in the kinematic equations developed in the study; the geometry interpolation and the deformation interpolation. The coupling between the rail deformation and geometry, contact coordinates, and nonlinear vehicle dynamics was considered. The main aim of the analysis was developing a new procedure that allows building complex track model used as an input to general purpose multibody computer program used in the dynamic analysis of railroad vehicle systems. This was achieved by the following consequence; first the track geometry was defined in a pre-processor computer program which produce an output geometry file including all information about the track elements of the space curve of the track and the left and right rail in terms of position coordinates and rotations defined at the selected nodal points, then making a finite element model of the track in a finite element pre-processor computer based on the track material properties and geometry and the output is a finite-element, finally the geometry file and the finite-element were used as an input to a general purpose multibody computer program in which the wheel-rail contact models are implemented to study the dynamic behavior of the railroad vehicle.

E. Meli et al. [17] has developed a numerical model which reproduce the complete three-dimensional dynamics of a railway vehicle running on a generic track. The model has been developed with the objective of real-time implementation, in order to use the results to control the actuators of Hardware In the Loop(HIL) test rigs. The numerical model in the test rig has been realized in Matlab–Simulink^{TM} environment. The module was applied to a benchmark vehicle (The Manchester wagon). Comparison between the obtained results and those obtained using a commercial multibody software package ADAMS/RAIL was shown. In the work presented by Meli et al, it was highlighted that the models used to evaluate the deformation of the wheel and the rail in the contact zone by means of two different approaches. With respect to the existing models of railway multibody models, its features were more detailed modeling of wheel-rail contact problems.

The step of the track geometry description represents the first step in the solution of the dynamic analysis problem in which the pre-processing operation for the track

geometry is made using the input data provided by the manufacturing or the industry to be the input for the track geometry program, then the output data generated in such step provided to the next step which include the multibody dynamic analysis program used to simulate the behavior of the rail guided vehicle. The track model used here in the dynamic simulation must be presented as a parameterized track in order to obtain the required information of the track and all the kinematic and dynamic parameters as a function of the parameter used here which is the distance covered by the vehicle or the track length, there is two main approaches used in the parameterization of the track centerline, the first one uses a combination of analytical segments, straight, transition and plane curve segments to form the track model used in the analysis. The second approach depends on the use of piece wise cubic interpolation schemes to make an interpolation between provided data points representing the track to find the parameterized track centerline curve. In both approaches it was necessary to define the cant angle of the track to provide a complete definition of the track. In the methodology presented in the work, it was proposed to use analytical segments to form the presented track; the track model presented in this work consists of tangent or straight line segment, followed by transition curve segment, and finally the plane curve segment with constant radius R. The pre-processed data defined in the track geometry step was provided to a multibody program used for the dynamic analysis of the railroad vehicle, starting with the study and the analysis of a general solid moving along the proposed track. As a next step the analysis of wheelset moving along the track and then the combination between the two solids in the step of the definition of the train vehicle model proposed in the work in the proceeding context. J. Pombo [22, 23] developed an appropriate methodology for the accurate description of the track centerline geometry, in the frame work of multibody dynamics. A pre-processing step was made to achieve the computational efficiency for the definition of spatial geometry of the centerline based on the data given by the user. Starting with the roller coaster application, four different interpolation schemes was used in the definition of the spatial track centerline. All the information and the data of the right and left rail was stored in a tabulated manner in which interpolation between the entries were made to obtain the required information. The application was extended to be used in the definition of railway track application in which the rail irregularities were implemented and piecewise interpolation schemes were used to parameterize the track irregularities as well as the input data, to obtain the track centerline as a function of the track length. Shabana et al. [29] use an analytical track description defined by three step procedure:

i) Projection, which define the planar curve obtained by projecting the track center-line onto the horizontal plane;
ii) Development, which defines an elevation angle;
iii) Super-elevation, which defines the track cant angle.

In his formulation, a relationship between the arc-length of actual curve and arc-length of the projected curve is stated. Then, the track centerline is defined by providing information about the horizontal curvature as a function of the projected

arc-length, the vertical development angle as a function of actual arc-length and the cant angle as a function of the projected arc-length. During the dynamic analysis, the rail space curve are obtained by means of absolute nodal coordinate formulation, leading to an isoperimetric beam element that can be conveniently used to describe curved rigid and flexible rails. The method considered each rail as a separate body in order to account for relative motion. The method used by Shabana [28] in the definition of the track pre-processing step, basically depends on the definition of the geometry file produced, the input data for this program use the industry data such as the curvature, super-elevation and development. The output data of the pre-processing stage was used in the next stage which is the development of a finite element pre-processor computer program. Description of the rail deformation was discussed which based on the finite element floating frame of reference formulation [25]. The use of this formulation allows for arbitrary rigid body displacement of the track structure, it also allows treating the two rails as one body or two separate bodies. The fundamental component common to all conventional railway vehicles is the wheelset [20]. The movement of the wheelset over the track is characterized by a complex interaction [4, 26] where lateral translation as well as yaw and roll rotations are observed. The formulation of the problem of contact between the wheel and the rail is complex task and has been the subject of several investigations which presented different solutions [21, 24, 27]. Two approaches can be used for solving the problem of wheel-rail contact in railroad dynamics. The first is the commonly called constraint approach, in which non-linear kinematic contact constraint equations are introduced. In this approach, the contact surfaces are represented in a parametric form using the differential geometry methods. The coordinates of the contact points can be predicted online during the dynamic simulation by introducing surface parameters that describe the contact surface geometries. The second is the elastic approach, in which the wheelset is assumed to have six degrees of freedom with respect to the rails. The local deformation of the contact surface at the contact point is allowed and the normal contact forces are defined using Hertz's contact theory or in terms of assumed stiffness and damping coefficients. This type of approach allows the separation between the wheel and the rail and allows multiple contact points to be managed. One of the main problems correlated with this approach is the definition of the contact point location online. In most elastic force models, the three-dimensional contact problem is reduced, for the sake of efficiency, to a two-dimensional problem when the location of the contact points is searched for. Both of these approaches allow the component of the contact force normal to the surfaces to be defined. In the constraint method these forces are calculated as the Lagrange multipliers that, together with the system generalized coordinate and the surface parameters time derivatives constitute the unknown vector of the differential algebraic equation system that describes the vehicle dynamics. In the elastic approach the normal component of the contact force at the contact point is calculated as a function of the penetration between the surfaces. The contact problem can be divided into three distinct but correlated tasks: the contact geometry, the contact kinematics, and contact mechanics. Contact geometry

is the problem of defining the location of the contact point on the profiled surfaces taking into account the geometric contact constraints which impose constraints upon the relative displacements and orientations of the contacting bodies. Contact kinematics defines the creepages (normalized relative velocities) at the point of contact. Contact mechanics determines the tangential creep forces and spin moment on the basis of three-dimensional rolling contact theories.

Shabana et al. [27] developed a new elastic force contact formulation for the dynamic simulation of the wheel-rail interaction. In this contact formulation, four surface parameters are introduced in order to be able to describe the geometry of the surfaces of the two bodies that come in contact. The method developed in the mentioned investigation exploits features of multibody computational algorithms that allow adding arbitrary first order differential equations. A differential equation associated with the rail arc length and expressed in terms of the wheel generalized coordinates and velocity is used to accurately predict the location of the points of contact between the wheel and the rail. This first order differential equation is integrated simultaneously with the dynamic equations of motion of the wheel-rail system, thereby defining the rail arc length traveled by the wheel. This arc length is used with an optimized search algorithm to determine all possible contact regions. Pombo [21, 24] presented a new general formulation for the accurate prediction of the location of the contact points on the wheel and rail surfaces. The mentioned model has been proposed and implemented in a general multibody program used in the dynamic analysis of railway vehicles. The coordinates of the contact points are predicted online during the dynamic analysis by introducing the surface parameters that describe the geometry of the contact surfaces. This method was applied to study specific problems inherent to the railway dynamics such as the two points of contact scenario. The methodology to look for the candidates for contact points is fully independent for the wheel tread and for the wheel flange. The used formulation also allowed for investigations related to hunting instability and prediction of wheel climbing, which are very important to study derailment phenomena. The methodology used [20] for the parameterization of the wheel and rail surfaces and for the description of the wheel-rail contact phenomenon was general, since it was able to represent any spatial configuration of the wheels and rails and any wheel and rail profiles, even the ones obtained from direct measurements. Because the wheels are treated separately, the used approach allowed dealing with railway vehicles either with conventional wheelsets, like trains, or with independent wheels, such as in many of the trams in operation.

In the contact model used by E. Meli et al. [17] the contact point position is calculated offline by means of a procedure based on the simplex method. This procedure was used to generate a three dimensional lookup table used in the real-time simulation to find the position of the contact points as a function of wheelset-rail relative displacement, described by three coordinates (the lateral wheelset

displacement, the roll and yaw wheelset angle). The procedure was numerically sufficiently efficient and allows multiple contact points to be managed. The method used here in solving the wheel-rail contact problem based on the elastic approach, in which the wheel is considered to have six DOF with respect to the rail and the normal contact forces are defined in terms of the indentation between the surfaces and using Hertz contact theory. The main problem encountered in when using the elastic approach, is the determination of the contact points. For sake efficiency, the three dimensional contact problem is usually reduced to a two dimensional problem [17] when searching for the contact points. In the dynamic analysis of railway vehicles, the evaluation of the wheel-rail contact forces is repeated many times. Then, short calculation time algorithm should be used taking the computational cost of the model implemented in the multibody computer program used in the analysis. The method used in the work here for calculating the tangential contact forces and moments is Kalker linear theory of rolling contact [12-15, 26], this theory based on the assumptions that the existence of small creepages and spin creep, and the area of slip is so small that its influence can be neglected. Under these assumptions, the adhesion zone is assumed to cover the entire area of contact. This method doesn't include the saturation effect of the friction force and, therefore, it is limited to contact problems with small creepage values. Due to the simplicity and computational implementation easiness, Cartesian coordinates are used [29] in this work to formulate the equations of motion of the multibody systems. No kinematic constraints are added to the formulation, to avoid the complexity produced from the Differential Algebraic Equations (DAE), also the instabilities in the integration process, produced from the substitution of the algebraic equations of the system by their counterpart (ODE), are avoided. Then the equations of motion developed in this work are set of Ordinary Differential Equations (ODE) solved by numerical integration algorithms. Two approaches are often used to formulate the dynamic equations of motion of mechanical systems: the Newtonian and the Lagrangian approaches. In the Newtonian approach, vector mechanics is used to develop the dynamic equations, in this approach the equilibrium position of each body is first studied separately, and it can be used relatively for simple systems and is not suited for the analysis of complex systems such as railroad vehicles. In the Lagrangian approach, scalar quantities such as the virtual work and the kinetic and potential energies are used to develop the equations of motion of the body. In this case there is no need to study the equilibrium of the bodies in the system separately [3, 29]. In this work the Lagrangian approach is used to develop the equations of motion of the multibody systems. The concept of the generalized coordinates is fundamental in the Lagrangian formulation of the equations of motion. For unconstrained motion proposed here in the formulation, six degrees of freedom are used for each body used in the multibody system; three coordinate are used to describe the translation of a point on the body and the other three are used to describe the orientation of the body frame of reference. The parameterization of the finite rotation used in this work is the set of Euler angles, where the orientation of a point on the rigid body is defined using three successive rotations. To avoid

singularity problems that may exist in the formulation, the final rotation in the successive rotations proposed was assigned to the higher values of rotation angles.

3 Chapter Three

Reference Frame description

3.1 Introduction

In this chapter the complete description of the reference frames is presented in order to give the detailed definition for all the variables and identities used in the mathematical representation of the models used in the dynamic simulation of the railway's multibody systems. This chapter also includes the definition of the system of reference used for the multibody computer program developed in this work. Each reference system is clearly defined, starting from the fixed reference frame, the track frame of reference which represent reference frame which follow the motion of the body [23,29]. The local coordinate reference frame of each body is introduced to represent the position and orientation of each point on the body with respect to each local frame. The origin and orientation of each local frame of reference is attached to the center of mass of the body. The transformation between the reference frames is defined by calculating the necessary matrix required, using the Euler angles with the sequence of rotation that avoid the singularity problem [29]. Cartesian coordinates are supposed to be used in the formation used due to the simplicity of its implementation in the multibody program used in the dynamic analysis of the railway vehicles, rotation sequences is defined for the track frame of reference, as a successive rotation about Z-axis, followed by rotation about Y-axis, and finally a rotation about X-axis. But for the rotation sequences used for the solid bodies it is defined as a successive rotation about Z-axis, then about X-axis and finally, the pitch motion with the rotation with about Y-axis.

3.2 Reference Frames.

In this section we would like to define all the frame of references used in the formulations, giving more details about each frame of reference used and its combination with the overall system. Starting with the description of the system used in the analysis of solid body as shown in fig (3.1), three main reference frames were defined, the first one is the fixed frame of reference (X Y Z), the second one is the track frame of reference (X_T Y_T Z_T) and the last one is the solid frame of reference (X_S Y_S Z_S).

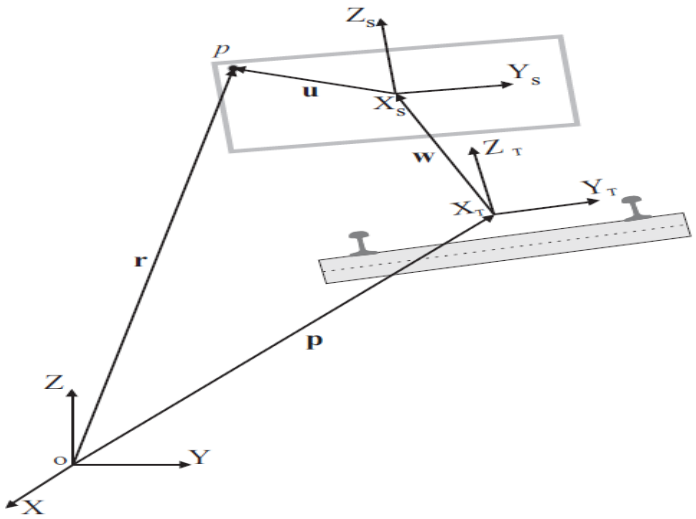

Figure 3- 1 Reference frame combination

3.2.1 Fixed Reference Frame

A system that can be located at any fixed point with respect to the system and bodies used in the analysis, which can be represented by a three orthogonal axes XYZ that are rigidly connected in one point called the origin O. The fixed frame of reference also called the global frame of reference. In this frame of reference all the measurable quantities that can define the configuration of the body can be represented with respect to it such as: displacement, velocities and acceleration. Fig 3.2 shows the global reference system consisting of three orthogonal axes Z, Y and X. the Z-axis point to the vertical direction, X and Y-axis forming the horizontal plane. A vector u is defined by three components that form u_x, u_y, and u_z. So the vector u can be written in terms of the component as follow:[25], since vector u is a unit vector and it should be a 3x1 matrix and not a 1x3 matrix, so it should be transposed.

$$u = [u_x u_y u_z]^T \qquad 3.1$$

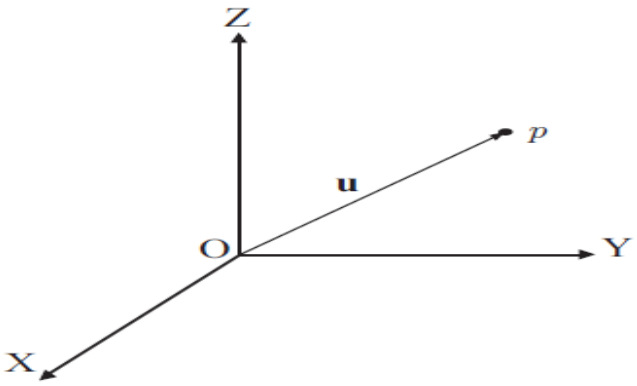

Figure 3- 2 Fixed reference frame

3.2.2 Track Reference Frame

Track reference frame here is defined with three orthogonal coordinate axes X_T, Y_T and Z_T as shown in figure 3.3. The track reference frame is located at the track center line presented between the left and right rail. The direction of the X_T axis pointing to the longitudinal direction referring to the rolling direction of the moving body along the track, Z_T axis pointing to the vertical direction normal to the track horizontal plane and the Y_T axis located normal to the two other axes of the frame.

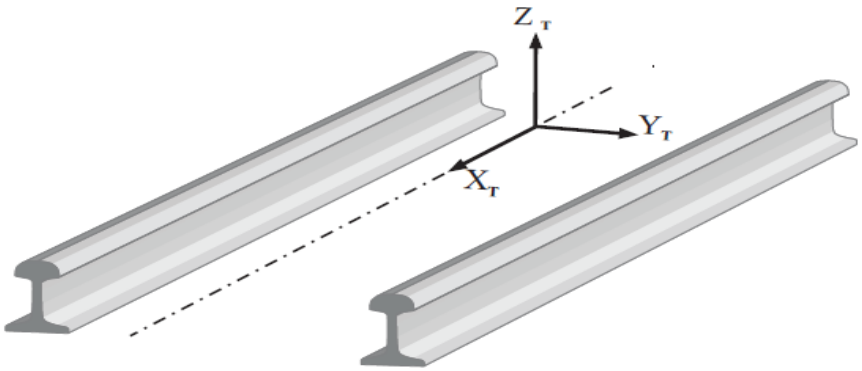

Figure 3- 3 Track reference frame

A point p located in the track reference frame has a position vector which can be expressed in the local track frame of reference as shown in figure 3.4.

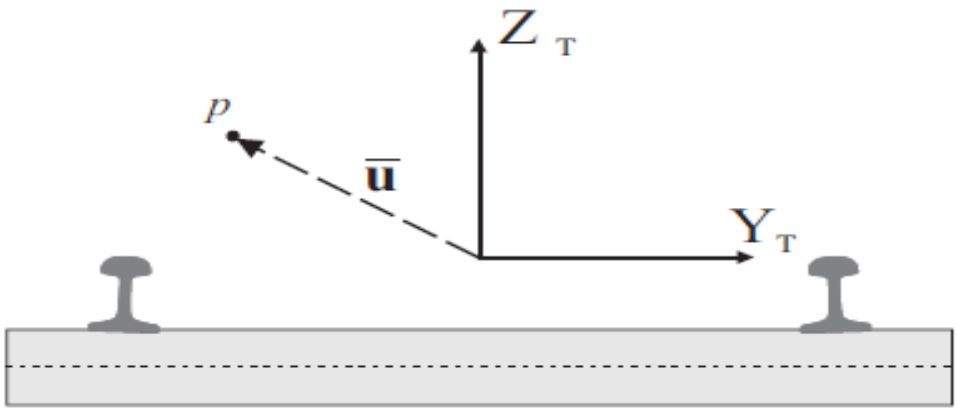

Figure 3- 4 Local position of point P in the track reference frame

$$\bar{u} = [\bar{u}_x \bar{u}_y \bar{u}_z]^T \qquad 3.2$$

In the expression it is noted that the use of the upper bar sign, means that the vector presented in the track local reference frame. This notation here was used to

distinguish the difference between the vector presented in the track frame of reference and the global frame of reference.

3.2.3 Solid Reference frame

As the track reference frame is presented; here the solid reference frame represented by three orthogonal coordinate axes X_S, Y_S and Z_S. The solid frame of reference is attached to the center of mass of the solid figure 3.5.

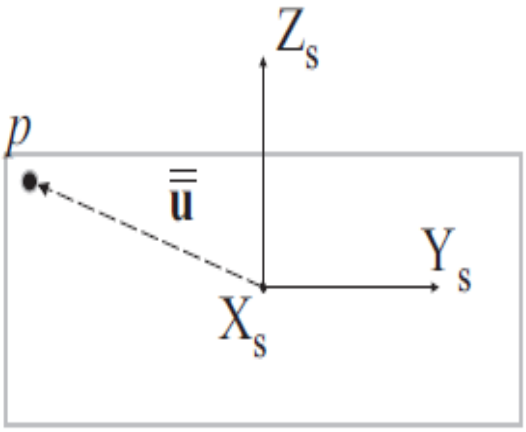

Figure 3- 5 Local position of point P in the solid reference frame

The local position vector of a point p located in the solid reference frame can be defined as

$$\bar{\bar{u}} = [\bar{\bar{u}}_x \, \bar{\bar{u}}_y \bar{\bar{u}}_z]^T \qquad 3.3$$

3.3 Reference Frame Transformation

In this part it is necessary to define how to make the transformation from one system to another in order to present necessary formulations used in the frames transformation in the proceeding chapters.

3.3.1 Transformation from Track to Fixed reference frame

Figure 3.6 shows the combination of the track frame (X_T $Y_T Z_T$) with the fixed or global reference frame (X Y Z). The global reference frame can be located at any fixed point selected by the user or the observer, and the track reference frame is located as it is appeared in the figure at the track center line between the right and left rail.

Point p in the track reference frame can be defined by the position vector, which represents the location of point p with respect to the fixed reference frame (X Y Z) and by the global position vector P, i.e.

$$r_p = P + U = P + A\bar{U} \quad 3.4$$

Where P, is the global position vector of the origin O_T of the track reference frame, U is the global position vector of the point *P* with respect to the fixed frame of reference. A is the transformation matrix for the track that defines the orientation of the track (X_T Y_T Z_T) frame with respect to the fixed frame (X Y Z). This matrix can be written as [25]:

$$A = A_z A_y A_x \quad 3.5$$

The selected sequence of rotation here is achieved by making three consecutive rotations about Z-axis and then about Y-axis and finally rotation about X-axis.

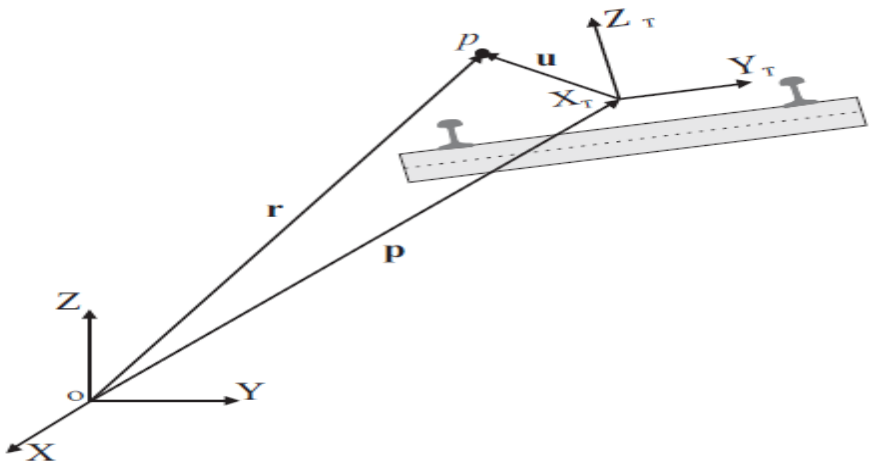

Figure 3- 6 Transformation from solid to track reference frame

For large rotation angles (orientation angle of point *p* with respect X Y and Z axes), the use of Euler angles in the calculation of the transformation matrix may cause singularity problems [4, 29]. To avoid this problems the selection of the rotation sequence for the track frame is chosen by making the largest rotation angle to be the final rotation, which is in our case here the rotation about X-axis representing the roll angle or the cant angle of the track [25]. The expression of the transformation matrix A illustrated in details in the included appendix.

3.3.2 Transformation from Solid to Fixed reference frame

The description of the transformation from the fixed frame of reference to the solid frame of reference illustrated here by defining the three main reference frames required to present the general solid which is in this case the body of the railway vehicle. Figure 3.7 shows the sequence of transformation from the global to the track reference frame, afterwards transformation from track to solid reference frame. Appoint *p* located on the solid body can be defining the position vector with respect to the global reference frame as:

$$r_p = P + w + u = P + A\bar{w} + AB\bar{\bar{u}} \qquad 3.6$$

Where $\bar{w}$ the position vector of the origin of the solid reference frame O_S, with respect to the track reference frame, B is the transformation matrix required to define the orientation of the solid reference frame ($X_S Y_S Z_S$) with respect to the track reference frame, and the position vector of point p with respect to the solid reference frame.

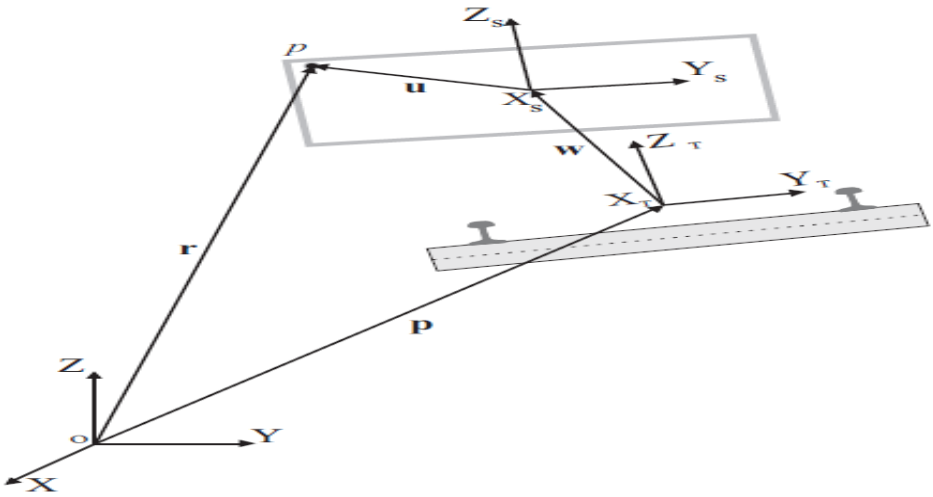

Figure 3- 7 Transformation from solid to fixed reference frame

The Transformation matrix B of the solid is obtained by three consecutive rotations using Euler Y-axis with an angle θ_y which represent the rotation of the wheelset. The selection of the rotation sequence here used to avoid the singularity problems that may be appeared in case of dealing with high values of the rotation angles during the motion.

3.4 Conclusions

Figure 3.8 illustrates the transformation from one system to another, to define the transformation matrices used in the analytical presentation of the identities used in the analysis of the railway dynamics. It appeared from the figure shown below, the matrix A is used to define the orientation of the track reference frame with respect to the global reference frame, and the matrix B is used to define the orientation of the solid frame of reference with respect to the track reference frame.

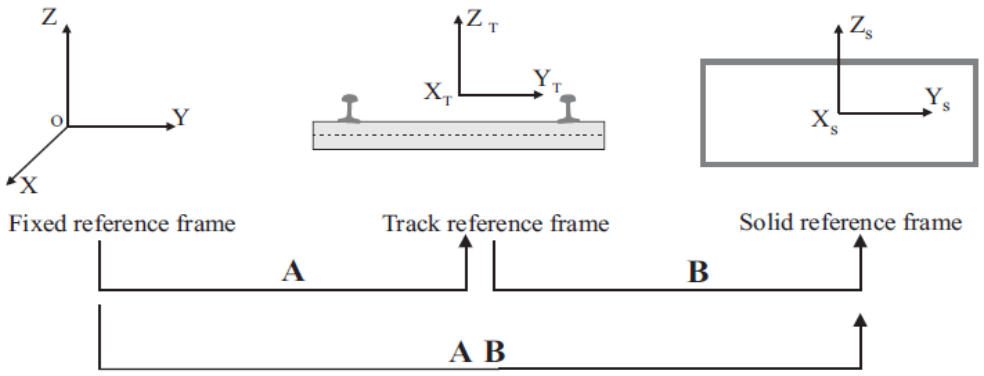

Figure 3- 8 Successive transformation between frames of references used

To define the orientation of the solid reference frame with respect to the global reference frame it is necessary to represent two successive transformations represented by the multiplication of the two matrices A and B respectively.

4 Chapter Four

Track Model

4.1 Introduction

The study of the rail road vehicle system and the dynamic analysis of railway vehicle system generally divided in to two main stages. The first stage is a pre-processing stage at which the track geometry and the wheel and rail profiles are defined. The second stage is developing the equation of motion of the multibody vehicle system, in this stage all the parameters required to define the wheel and rail profiles are defined as well as the track geometry parameters which enter the formulations of the contact conditions and the system equations of motions. Thus as a first stage here in the methodology proposed for the analysis of the rail road vehicle, the paper have to define the track geometry and make modeling for the track to provide the required data in the next step of the dynamic analysis of the problem [29]. Any track irregularities can be perceived as deviation from the reference path parallel lines, representing the track rails, the introduction of the track irregularities is not considered here in this work. The track models for multibody analysis must be in the form of parameterized curves, where the nominal geometry is obtained as a function of a parameter associated to the track curve length [21, 23]. The parameterization of the track can be done in two approaches, the first approach is the use of analytical segments for the track parameterization including the definition of the track generally done by putting together straight and circular curves interconnected by transition track segment that insure the continuity of the first and second time derivative of the railway in the transition points. The second approach depends on the parameterization of the track using parametric curves such as Akima splines [1] shape reserved splines and piece wise cubic interpolation schemes. These methods require the definition of data points representing the track and provide the interpolation between these points to represent the parameterized track path. Undesired oscillations produced with using the mentioned interpolation schemes and this can be avoided in such case of the horizontal track geometry for railway application, by the use of analytical segment.

4.2 Track Characterization

The primary dynamic inputs to railway vehicles come from track geometry variations. In order to study vehicle-track interaction and to evaluate track quality, vehicle performance and loading conditions should be investigated. It is necessary to represent the track geometry accurately [5]. The track pre-processor uses industry input data such as the curvature, super-elevation and development [28]. Then all the necessary data required as input information for the track model, will be provided in a separated input data file, and then the output data of the track geometry programs will

be provided to the dynamic simulation program. This step of obtaining the required data as a pre-processing data provided rapidly.

4.3 Track Geometry

The performance of the railway vehicle is dependent, on a great extent, of the track conditions. The loads included on the vehicle by the track and corresponding forces transmitted to the track by the vehicle also depends on the track geometry. In this section, some physical aspects relevant for the design geometry of the track are presented.

4.3.1 Track Gauge

The track gage is defined as the distance G between the inner edges of the rail heads, measured 12 mm below the track plane, as shown in Fig. 4.1. The standard gauge track has a value of 1435 mm.

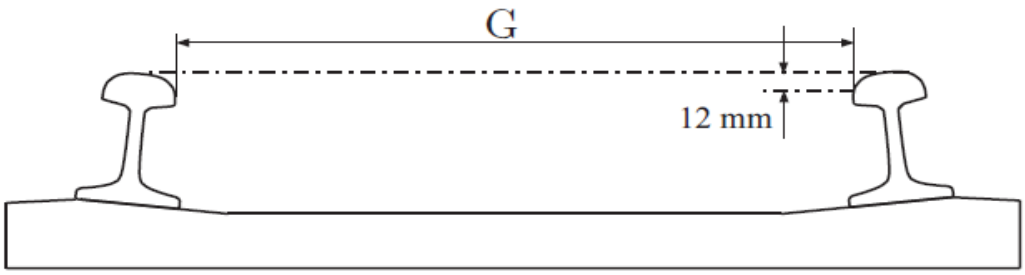

Figure 4- 1 Track gauge description

4.3.2 Horizontal Curves

The railway tracks are in general composed of straight (or tangent) sections, transition curves and circular curves. The horizontal curves have constant radius and are defined in the tracks described in the horizontal plane. The radius of the curve used is defined with respect to the track centerline as shown in Fig. 4.2.

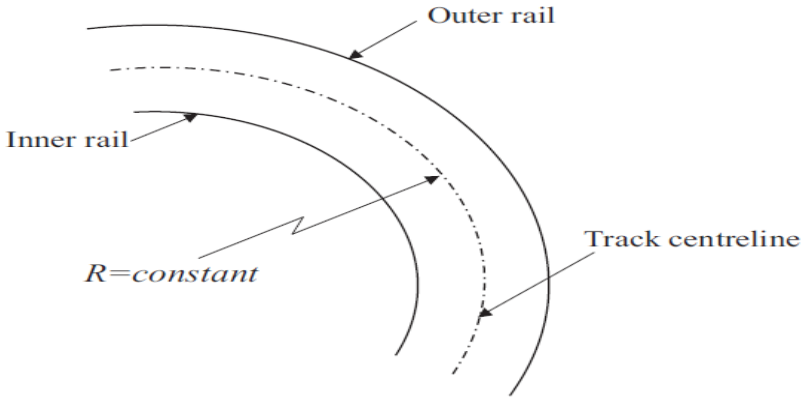

Figure 4- 2 Horizontal circular curve

4.4 Cant Angle Definition in the track model

4.4.1 Cant and Equilibrium Cant

When traveling in horizontal curves, railway vehicles are influenced by centrifugal forces, which act in a direction way from the center of the curve to overturn the vehicle. The sum of a vehicle weight and its centrifugal forces produced a resultant force directed to the outer rail. In order to counteract this force, the outer rail in a curve is raised [9, 20, and 29]. The difference in height between the outer and the inner rail plane is called the cant or the super elevation h_t, which can be defined as shown in Fig. 4.3

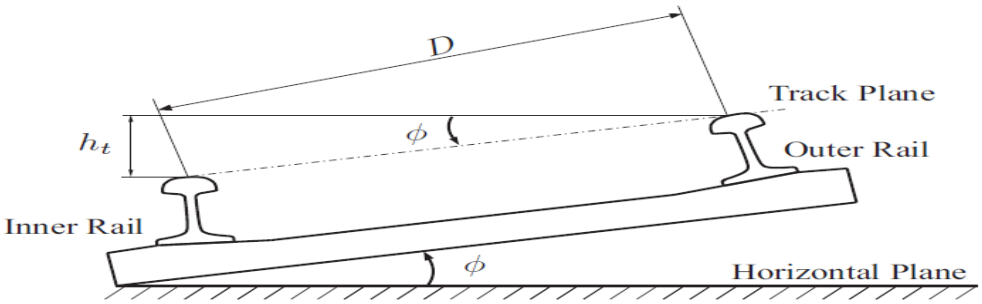

Figure 4- 3 Cant and cant angle

Then the cant angle ϕ as shown in the figure can be defined as [20, 29]

$$\phi = arcsin\left(\frac{h_t}{D}\right) \tag{4.1}$$

The cant angle of zero track plane acceleration, at a given radius of curvature R and vehicle speed V can be defined as equilibrium cant angle [20] which can be found by

$$\phi_{eq} = arctan\left(\frac{V^2}{Rg}\right) \tag{4.2}$$

To define the track cant angle first the plane at which the cant angel defined should be defined. So in the case of the flat tracks, the horizontal plane is the plane at which the cant angle is defined with respect to it. But in case of the full spatial geometry track model it is proposed to use the osculating plane Fig. 4.4, to be the reference plane at which the cant angle should defined [21, 23].

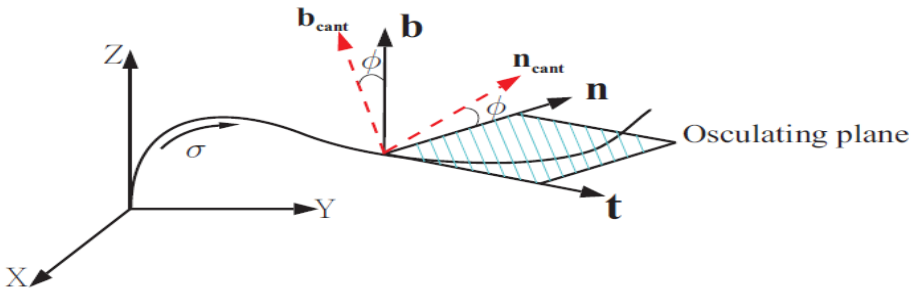

Figure 4- 4 Frenet principle vectors and special definition of the cant angle

In this section the definitions of the principle vectors (t n b) [17, 23] may be used, which are the tangent, normal, and binormal vector respectively defining Frenet frame that is attached to the spatial curve presenting the track centerline and the tangent, normal and binormal unit vectors can be found. Finding the relations between them after the rotation with the cant angle (ϕ), the vectors will be defined as (t_{cant} n_{cant} b_{cant}). It has to be said that if piecewise cubic interpolation was used to make the parameterization of the spatial curve then the user must set the cant angle corresponds to each one of the nodal points that is used to parameterize the track. If it is supposed to use the analytical representation of the track model using analytical functions the user must set the cant angle at the extremities of each track segment [20, 21]. In the case here the cant angle can be defined by the angle of rotation of the track frame of reference about the X_T-axis pointing to the direction of motion of the railway vehicle Fig.4.5

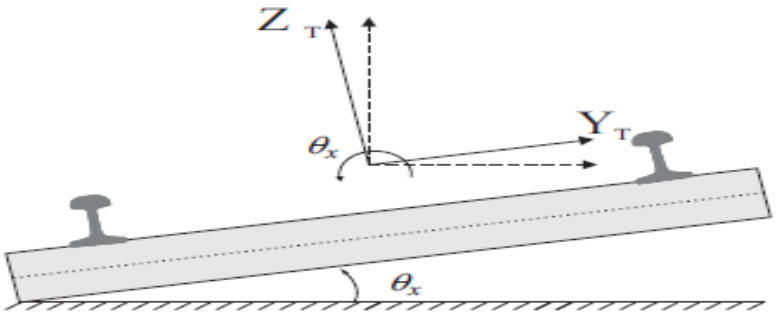

Figure 4- 5 Railway track cant angle

It is supposed here in the analysis to use the transformation matrix A which is used to transform from the Track frame to the Fixed frame of reference, this matrix is obtained from a set of successive rotations as defined in chapter.(3).

4.4.2 Transition Curves and Super-elevation Ramps

When trains operated at normal speeds, a circular curve with cant cannot be followed directly by a tangent track, and vice-versa [20]. A transition curve is needed to guarantee the curvature continuity and minimize the change in the lateral acceleration

of the vehicle. In general transition curves and super-elevation ramps Fig. 4.6 have the same start and the same end points. i.e., the curvature and the cant in transition curves correspond to each other. The length of the transition curves varies directly with the amount of curve super-elevation required. The maximum allowable rate of change of the super-elevation determines the minimum length of the transition for a given vehicle speed and curve super-elevation. The figure illustrates the main stages used in the simulation proposed here. R is the radius of curvature used in each stage which has an infinite value for the straight track and increases during the transition stage until it reaches the constant value at the circular curve stage as shown. h_{to} and h_{tmax} are the height of the track in the straight stage and the final or circular curve stage respectively.

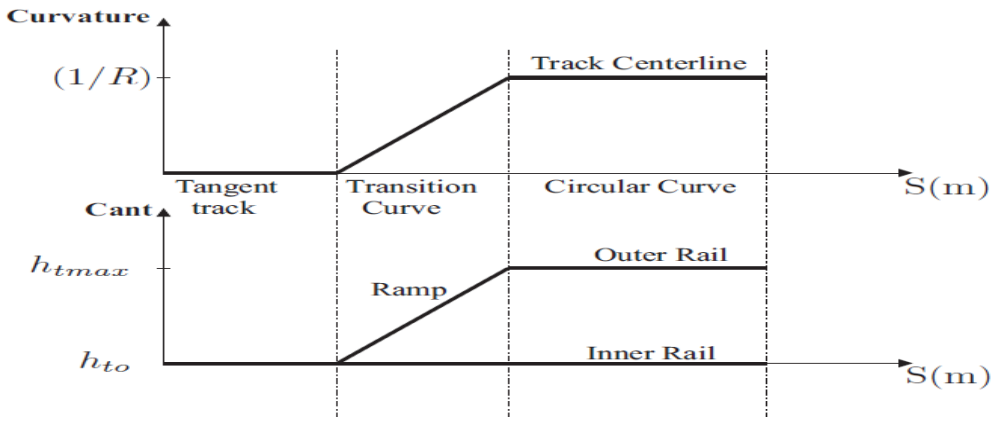

Figure 4- 6 Transition curve and super-elevation ramps

4.5 Track Geometric Descriptions

The dynamic analysis of any railway guided vehicles requires an accurate description for the track geometry [6, 20]. The track is composed of two rails defined in a plane that sits in the track centerline spatial curve, also called the reference path. The basic ingredient to define the track is to define the geometry of the reference path which must include, vertical gradients, horizontal curves and cant angle. The objective of this part is to introduce a complete description for the geometrics features of the track, and to present their computational implementation in a suitable form for the multibody methodology used in the analysis of the railway systems. For railways and light track vehicles the description of the nominal geometry of the track is generally done by assembling straight and circular segments together, interconnected by transition segments to ensure continuity of the first and second derivatives of the railway in transition points. To ensure smooth variation of the lateral accelerations of the vehicle during the change from the straight, or tangent, track to circular track or the change from circular path to straight one, the complete characterization of the track requires the definition of the cant angle variation along the reference path [9, 29]. For flat tracks, the cant angle is defined as the angle between the horizontal plane

and the rails plane, but for spatial geometry, the definition of the cant angle is proposed to be the angle between the osculating plane and the rails plane.

4.5.1 Parameterization of the track centerline

4.5.1.1 Overview of the track pre-processor

For the parameterization of the track centerline model first the approach used in the parameterization procedure should be defined. One of the most commonly used approaches is the use of analytical segments [22, 23] for representation of the track parameters, and in this procedure the track has to be defined or built using a combination of tangent track, transition curve and circular curve segments. The second approach that can be used is the parameterization of the track centerline using parametric curve interpolation schemes [20, 23], between the control points that can be used as an input data, defined by the user and the corresponding cant angle at each point. Once the approach for the parameterization procedure is clearly defined, then centerline can easily be parameterized as a function of the distance covered by the vehicle (σ), also the cant angle parameterized as function of the track distance covered by the vehicle (σ) and the frame of reference associated to the track centerline after the cant angle rotation can be calculated. So the procedure can be summarized in the following steps:

- Definition of the approach used for parameterization of the track centerline whether it is analytical segments or piecewise cubic interpolation scheme, this is defined by the user.
- Once the approach is selected then the track centerline is parameterized as function of the covered distance (σ) presenting the distance covered by the railway vehicle during the simulation.
- The cant angle also parameterized also as a function of the distance covered by the vehicle, and then we can define the frame of reference associated to the track centerline after the cant angle rotation.
- An output database is defined to all the necessary parameters required to define the track centerline geometry stored in it, and this database file is used as an input to the dynamic multibody code.

The method used here in the representation of the track model use the analytical segments [17, 20, 22] approach make parameterization of the track centerline, so the track here as described below in the following context. Using a combination of tangent or straight line segment, followed by transition curve segment to ensure the smooth transition between the tangent part and the circular curve segment.

4.5.1.2 Track modeling using analytical Segment

In this part the specification of the track used in the dynamic simulation is given, the mathematical presentation of the track at each point represented in the section below to give position vector and then all the kinematic variables at each distance (σ) on the track .The track segments will be selected as the following order:

I. Straight line track, followed by
II. Transition curve, and then
III. Circular curve with constant radius

IV.

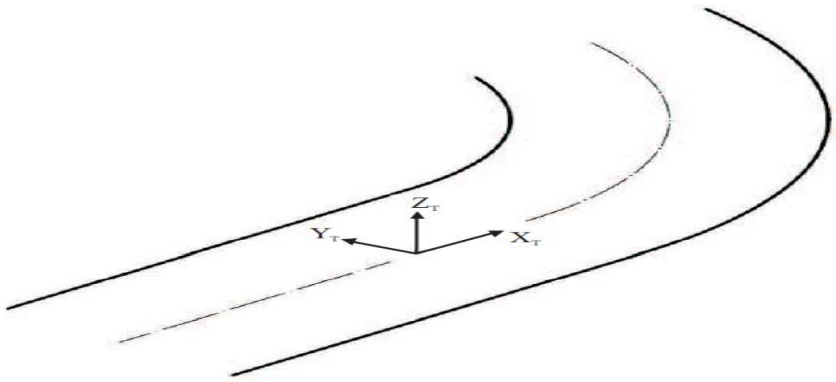

Figure 4- 7 Track model used in the dynamic simulation

The track reference frame represented by the three orthogonal axes (X_T Y_T Z_T) will be assigned to the centerline between the left rail and the right rail as shown in Fig. 4.7, where the X_T axis is pointing to the rolling direction or the movement direction of the railway vehicle as it was defined in the previous chapter of the definition of the reference frames which can be shown by the following Fig.4.8; representing the steps of the track

1. Straight line stage

The track presented here starts with a straight (or tangent) segment as shown in Fig.4.9. The starting point of the straight segment of the track is the distance point σ = 0, and the end point of the straight segment is the point σ = l_1, This can be represented by the simple straight line equation of first order as

$$x(\sigma) = a_s(\sigma) + b_s \qquad 4.3$$

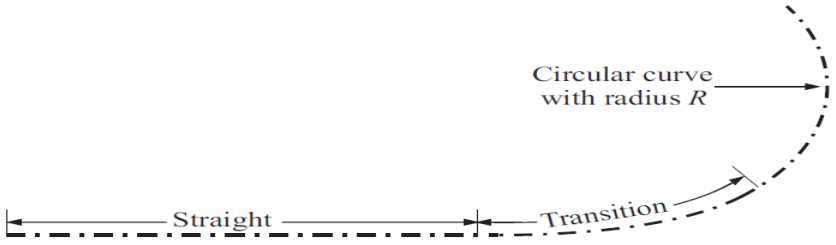

Figure 4- 8 Track segment definition

Where: a_s, b_s are constants of the straight line equation. This stage was considered to be the first stage in the track simulation. Then the track can be parameterized as a function of the track distance covered as

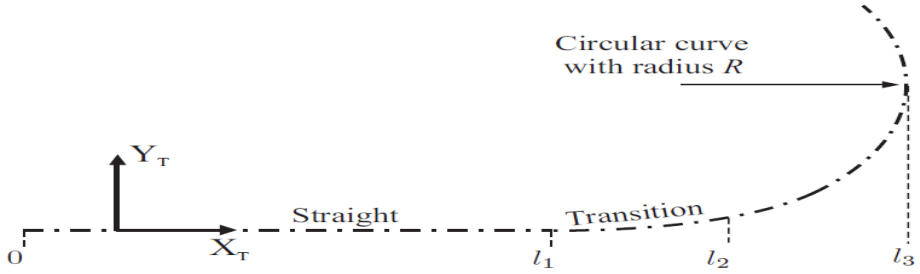

Figure 4- 9 Track segment length

$$s(\sigma) = \begin{bmatrix} x(\sigma) \\ y(\sigma) \\ z(\sigma) \end{bmatrix} \quad 4.4$$

Substituting with the values of $\sigma = 0$ at the beginning of the straight stage and $\sigma = l_1$ at the end of the straight stage we found that, also with substituting with the value of the cant height for obtaining the z position at the straight track stage we find that

$$x(\sigma) = \sigma \quad 4.5$$

$$z(\sigma) = h_{to} \quad 4.6$$

then the position vector of a point on the track in the straight line stage can

$$s(\sigma) = \begin{bmatrix} \sigma \\ 0 \\ 0 \end{bmatrix} \quad 4.7$$

2. Transition Curve stage

The transition curve is called mathematically Euler spiral, fitted between a straight line and circular curve. The transition curve starts with a radius equal to the infinity and ends with a radius equal to the radius of curvature of the adjacent curve. In our analysis here, a transition curve of the type clothoid is used as shown in the Fig.4.10.

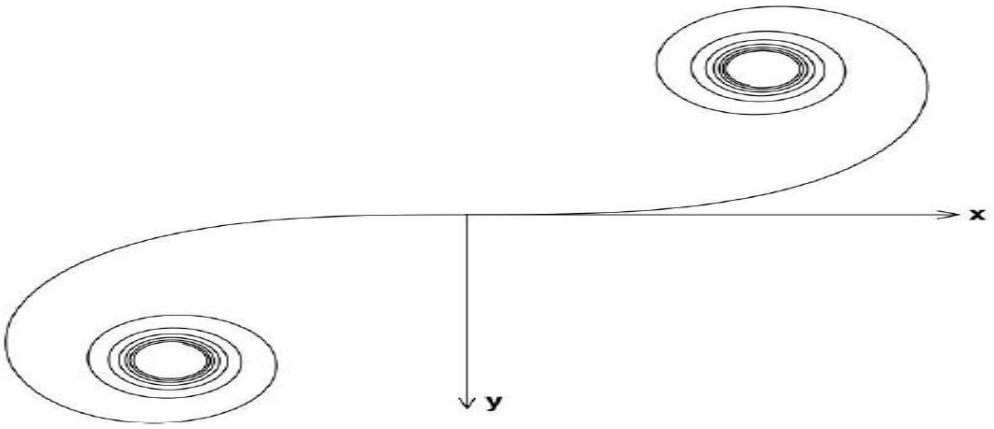

Figure 4- 10 Transition curve represented by clothoid curve

The transition curve here represented by the clothoid curve interconnects the straight and circular tracks to ensure the continuity in the first and second derivatives of the railway in the transition points, the transition curves are responsible for smooth variation of the lateral acceleration of the vehicle, when it moves from a straight track to a circular track or between two track segments of the same type with different radius or orientation [23]. To represent the transition between the straight line stage and the circular curve or the circular stage transition curve should be available. The tracing method used for the transition curve used is the conserved radius method, which leads to the parabolic equation of the clothoid obtained given by the following expression [23].

$$y = \frac{x^3}{6 l_{clo} R} \tag{4.8}$$

Where l_{clo} is the clothoid length, and R is the radius of the circular curve of the following stage. Using Fresnel integral coordinates of the clothoid can be represented as a function of the distance σ as follow

$$y(\sigma) = \frac{1}{6}\sigma^3 K - \frac{1}{84}\frac{\sigma^7}{\pi^2}K^3 \tag{4.9}$$

Where: K is a constant can be calculated as

$$K = \frac{1}{l_{clo}\, R} \tag{4.10}$$

The transition curve in our simulation will start at the point $\sigma = l_1$ and will end at the point of connection to the constant radius curve at the point $\sigma = l_1 + l_2$, where l_2 is the clothoid length l_{clo} . As it was shown it was necessary, for the parameterization method used here in the track parameterization using the analytical segment approach

to define the cant at the starting and at the end of each stage. So for the transition cure stage here represented by the clothoid the height at the beginning h_{to} and at the end of the stage h_{tmax} can be found, and assuming linear cant through the transition stage we find that the elevation of any point on the track can be found by

$$z(\sigma) = h_{to} + \frac{h_{tmax} - h_{to}}{l_{clo}} \tag{4.11}$$

Knowing that the value of h_{to} is equal to zero in case of the straight track, then the position vector of any point on the clothoid curve can be written in matrix form in the planer representation as follow

$$s(\sigma) = \begin{bmatrix} \sigma - \frac{1}{10}\frac{\sigma^5}{\pi^2}K^2 \\ \frac{1}{6}\sigma^3 K - \frac{1}{84}\frac{\sigma^7}{\pi^2}K^2 \\ \frac{h_{tmax} - h_{to}}{l_{clo}}(\sigma) \end{bmatrix} \tag{4.12}$$

3. Circular Curve stage

This is the third stage in the simulation of the track geometry, in this stage the track take a circular path with a constant radius of curvature R, the stage will start at the end point of the clothoid which can be assigned to the point $\sigma = l_1 + l_2$, and will end at the point at which $\sigma = l_1 + l_2 + l_3$, where l_3 is the circular curve length . The circular curve initiation point related to the previous stage as we know that the final point of the clothoid stage is same initiation point of the circular curve stage, so by defining the clothoid angle that can be written as

$$\Phi(\sigma) = arctan\left(\frac{dy/d\sigma}{dx/d\sigma}\right) \tag{4.13}$$

As a conclusion the initiation angle of the circular curve is the angle of the clothoid when the value of σ is equal to the clothoid length l_{clo} and this can be represented as

$$\Phi(\sigma) = \Phi(\sigma = l_{clo}) \tag{4.14}$$

Then the angle of the circular curve segment at any point σ on the circular curve, can be calculated from the expression

$$\Phi_p = \Phi(\sigma) + \frac{\sigma}{R} \tag{4.15}$$

Where: R is the radius of curvature of the circular curve segment. The position vector of the initiation point of the circular curve indicated by the subscript i, so it can be written as

$$x_i(\sigma) = x(l_{clo}) \quad 4.16$$

$$y_i(\sigma) = y(l_{clo}) \quad 4.17$$

Finally we can write the components of the position vector of a point on the circular curve indicated by the subscript *P* as follow

$$x_p(\sigma) = sin\left(\frac{\sigma}{R} + \Phi_i\right) - \sin(\Phi_i)\, R + x_i \quad 4.18$$

$$y_p(\sigma) = -cos\left(\frac{\sigma}{R} + \Phi_i\right) + cos(\Phi_i)\, R + y_i \quad 4.19$$

$$z_p(\sigma) = h_{tmax} \quad 4.20$$

$$s(\sigma) = \begin{bmatrix} x_p(\sigma) \\ y_p(\sigma) \\ z_p(\sigma) \end{bmatrix} \quad 4.21$$

4.6 Conclusion

The parameterization method used here ensure the representation of all the track geometric properties as a function of the distance covered by the vehicle σ, a pre-processor data file is generated containing all the geometrical properties of the track. This methodology guarantee that the time required for the dynamic simulation of the rail guided vehicle completely independent of the track complexity and the type of the scheme used for parameterization. But the paper have to mention that the use of analytical segments [22, 23] for the parameterization process, especially for the horizontal tracks which is not having large complexity, has a great advantage which it doesn't produce any undesired oscillations in the track model but the only disadvantage of this method is the fact that it cannot be used for the geometries which containing vertical curvatures, so it is only applied for horizontal track models. Reaching to this point, one can obtain all the information and the data related to the track designed for the simulation issues, including the position, velocity and acceleration vector of any point with respect to the fixed frame. Also the transformation matrix required to transform from track to fixed reference frame was obtained, the angular velocities related to the track reference frame also have been obtained at each stage of the track.

5 Chapter Five

Multibody System Methodology

5.1 Introduction

Multibody methodologies are not widely used despite the fact that such methodologies can be applied to develop more detailed and general models for railroad vehicle-track systems [26]. In the proceeding context of this chapter, the geometric, kinematics and dynamic aspects of a general solid system moving along parameterized track representing the railroad were discussed. Equations of motion presenting the multibody systems were formulated for a system consists of multiple rigid bodies each with six DOF, avoiding the use of any kinematic constraint on the motion in order to overcome the difficulties produced when using of the kinematic constraints which appeared in the need to solve a set of differential algebraic equations [20, 23] or the transformation of the system of differential algebraic equations (DAE) to ordinary differential equations (ODE), and then the use of stabilization techniques for the constraint equations in the solution was also avoided. The fundamental component common to all conventional railway vehicles is the wheelset. In general, it consists of two coned wheels rigidly fixed to a common axle. The movement of the wheelset over the track is characterized by a complex interaction where appreciable lateral translations as well as yaw and roll rotations are observed. The simulation of railroad vehicle-track systems using multibody computer algorithms requires the use of a module for the wheel-rail interaction [4, 16]. This interaction, which is due to the rolling and slipping contact between the profiled surfaces of the rail and wheel, has a significant effect on the vehicle dynamics and stability [26]. Contact point position was detected in the formulation presented in this chapter, the velocity vector of the contact point was calculated and then the creepages introduced at the wheel-rail contact point were determined. Forces due to contact including the normal contact force and the tangential forces are calculated. The moment vector at the contact patch was calculated, using an alternative technique, in which the contact moment is replaced with equivalent pair of forces of equal magnitude and opposite directions, acting on a plane perpendicular to the direction of the moment [11], and both supposed to be acting through the longitudinal direction. Then the force vector applied to the wheelset at contact point is determined in order to be implemented in the MBS program used in the dynamic simulation vehicle systems. An important term in the methodology proposed, is the determination of the force vector applied to the bodies produced from the spring element connecting two rigid bodies. Translational force element is used connecting two bodies, this element can consist of a spring, a damper, and an actuator. The coefficients used in this element formulation to define the forces can be linear or nonlinear functions of the relative motion and velocity of the two bodies connected by this element; in our case here linear functions are used. Lagrangian approach was used here to determine the

equation of motions of the system, it is mainly depends on the definition of the generalized coordinates of the system and the determination of the generalized force vector affecting the body under study. Kinematic analysis of a general solid was presented followed by the dynamic analysis of such solid, and then the formulations extended to include the kinematic and dynamic analysis of the wheelset including the definition of the normal contact forces, creepages and tangential contact forces at the contact patch resulting from the wheel-rail interaction.

5.2 Equations of Motion of general solid body system

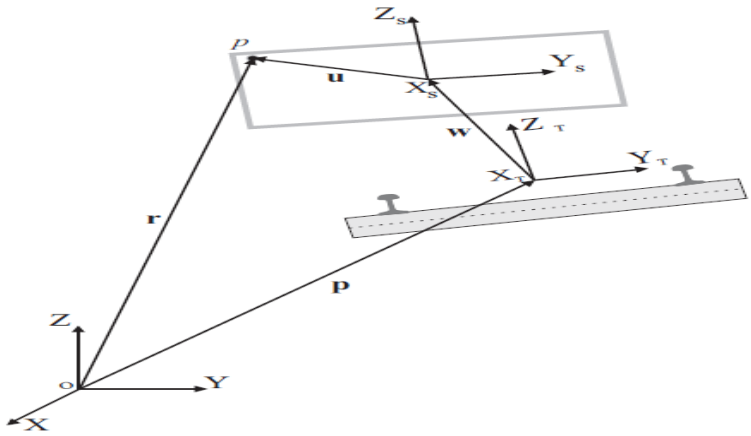

Figure 5- 1 General solid body with respect to global reference frame

In this part the paper would present the formulations that can be used to calculate the position vector of arbitrary point located on a solid body using the relations developed in chapter 3 like the position vector of an arbitrary point on solid or wheelset, the velocity vector and finally the equations of motion of the system can be obtained. The method that will be used in the calculation of the equations of motion is Lagrangian method for the development of the system equation of motion, and then defining the forces affecting the solid and the determination of the generalized forces associated with the system generalized coordinates [25, 29]. In the Lagrangian approach, scalar quantities such as the virtual work and the kinetic and potential energies are used to develop equations of motion of the body without studying the equilibrium of the bodies in the system separately. But to use Lagrangian approach first the position and velocity vector of the system (kinematics of the system) should be computed.

5.2.1 Kinematic analysis of solid body system

The kinematic analysis consists of the study of the motion of the system independently of the forces that cause it. The kinematic analysis is done to obtain the system position and velocity vectors and determination of the generalized coordinates of the system under study [3, 25]. Reaching to this point, we can define the position vector of a point located on the solid body as shown in Fig. 5.1 using equation (3.6).

And by making the first time derivative for the position vector, we can obtain the velocity vector of an arbitrary point located on the solid as

$$\dot{r}_p = \dot{P} + \dot{A}\bar{w} + A\dot{\bar{w}} + (\dot{A}B + A\dot{B})\bar{\bar{u}} \quad 5.1$$

where $\dot{r}_p$ is the velocity vector of an arbitrary point p, $\dot{P}$ is the velocity of the origin of the track system of reference, $\dot{A}$ first time derivative of the transformation matrix required to transform from the track frame of reference to the fixed frame of reference1 , $\dot{\bar{w}}$ is the velocity of the origin of the solid reference frame which represent the velocity of the CM of the system as the solid reference frame was defined to be coincided with the solid inertial frame of reference located in CM, $\dot{B}$ is first time derivative of the transformation matrix required to transform from the solid frame of reference to the track frame of reference .

5.2.2 Total Kinetic energy of the system

Referring to the kinetic energy equation presented in bibliography [25], the kinetic energy of a solid body can be written as

$$T = \frac{1}{2}\int \rho \dot{r}^T \dot{r} dV \quad 5.2$$

Where ρ and V are respectively the mass density and the volume of the body, then the kinetic energy can be written as. Integrating Eq.(5.2) with respect to volume will give

$$T = \frac{1}{2}\dot{q}^T M_s \dot{q} \quad 5.3$$

Where q is the vector of the generalized coordinates of the solid body given by the following equation

$$q = [\bar{w} \quad \theta]^T \quad 5.4$$

Where w is the vector of displacements of the solid reference frame, and θ is the vector of the rotation angles determining the orientation of the solid. According to the portioning of the generalized coordinates of the solid body, the kinetic energy can be found by the following equation

$$T = T_{\bar{w}\bar{w}} + T_{\bar{w}\bar{\theta}} + T_{\bar{\theta}\bar{\theta}} \quad 5.5$$

where T is total kinetic energy of the solid, $T_{\bar{w}\bar{w}}$ is the translational kinetic energy term, $T_{\bar{w}\bar{\theta}}$ represents the coupling between the translational kinetic energy and the rotational kinetic energy term, and $T_{\bar{\theta}\bar{\theta}}$ is the rotational kinetic energy term. But for the solid body system presented in such case, the term that represents the coupling

between the translational and rotational kinetic energy $T_{\bar{w}\bar{\theta}}$, is null because the solid frame of reference (X_S Y_S Z_S) is located at CM of the solid body. Then total kinetic energy of the system in this case will be written as

$$T = T_{\bar{w}\bar{w}} + T_{\bar{\theta}\bar{\theta}} \quad 5.6$$

5.2.3 Translational Kinetic energy of the system

The translational kinetic energy term of the solid body can be written as

$$T_{\bar{w}\bar{w}} = \frac{1}{2}\dot{r}_{CM}^{T} M_s \dot{r}_{CM} \quad 5.7$$

Where r_{CM} is the position vector of the center of mass of the solid body represented by

$$r_{CM} = P + A\bar{w} \quad 5.8$$

and M_s is the mass matrix of the solid body can be written as

$$M_s = m_s I_{3x3} \quad 5.9$$

The vector representing the velocity of the center of mass point, can be found through the equation

$$\dot{r}_{CM} = \dot{P} + \dot{A}\bar{w} + A\dot{\bar{w}} \quad 5.10$$

Substituting in the translational kinetic energy term Eq.(5.7) obtained

$$T_{\bar{w}\bar{w}} = \frac{1}{2}\dot{P}^T M_s \dot{P} + \left(\dot{P}^T + \frac{1}{2}\dot{\bar{w}}^T A^T + \bar{w}^T \dot{A}^T\right) M_s A\dot{\bar{w}} + \left(\dot{P}^T + \frac{1}{2}\bar{w}^T \dot{A}^T\right) M_s \dot{A}\bar{w} \quad 5.11$$

5.2.4 Rotational Kinetic Energy of the system

The rotational kinetic energy of the solid can be written as

$$T_{\bar{\theta}\bar{\theta}} = \frac{1}{2}\bar{\bar{\omega}}^T J_{\theta\theta}\bar{\bar{\omega}} \quad 5.12$$

where $J_{\theta\theta}$ is the inertia matrix of the solid1, ω is the angular velocity of the solid represented in the solid reference frame which can be written as

$$\bar{\bar{\omega}} = \bar{\bar{\tau}} + \bar{\bar{L}}\dot{\theta} \quad 5.13$$

where $\bar{\bar{\tau}}$ is the track angular velocity vector represented in the solid reference frame, the term $\bar{\bar{L}}\dot{\theta}$represents the relative angular velocity of the solid with respect to the track frame of reference, and L is the matrix containing the vectors acting through the rotation axes Z_S , X_S , and Y_S respectively which are defined in the global reference

frame1 and it represents the matrix that relates the absolute angular velocity vector of the rail to the time derivatives of the orientation parameters [28]. By substitution in the rotational kinetic energy Eq. 5.12 we found that

$$T_{\theta\theta} = \frac{1}{2}\bar{\bar{\tau}}^T J_{\theta\theta}\bar{\bar{\tau}} + (\bar{\bar{\tau}} + \frac{1}{2}\dot{\theta}^T\bar{\bar{L}}^T)J_{\theta\theta}\bar{\bar{L}}\dot{\theta} \qquad 5.14$$

By substitution Eq.(5.11) and Eq.(5.14), on Eq.(5.6) the total kinetic energy term represented be found by

$$T = \frac{1}{2}\dot{P}\ \ M_s\dot{P} + \left(\dot{P}^T + \frac{1}{2}\dot{\bar{w}}^T A^T + \bar{w}^T\dot{A}^T\right)M_s A\dot{\bar{w}} + \left(\dot{P}^T\ \ + \frac{1}{2}\bar{w}^T\dot{A}^T\right)M_s\dot{A}\bar{w} + \frac{1}{2}\bar{\bar{\tau}}^T J_{\theta\theta}\bar{\bar{\tau}} + \left(\bar{\bar{\tau}}^T + \frac{1}{2}\dot{\theta}^T\bar{\bar{L}}^T\right)J_{\theta\theta}\bar{\bar{L}}\dot{\theta} \qquad 5.15$$

5.3 Dynamic analysis of solid body system

The dynamic analysis of multibody systems consists of the study of their motion as response to the external applied forces and moments [2, 11, 25]. The motion of the system is generally not prescribed, being its calculation one of the principle objectives of the dynamic analysis. This type of analysis also provides a process to estimate external forces that are dependent on the relative position between the system components, such as those type of forces generated by springs, dampers and actuators. Also the external forces generated as a consequence of the interaction between the system and its surrounding environment, such as contact and friction forces are considered [20].

5.3.1 Equation of motion of the solid body

In this section, the dynamic equation of motion of solid body treated as a rigid body is derived. To determine the configuration of the solid body system, it was first necessary to define generalized coordinates q as defined in the previous section of the kinematic analysis [29], that specify the position and orientation of each point of anybody in the multibody system presented by the solid system shown in Fig.5.1.

5.3.2 Lagrange's equation of motion

In the Lagrangian approach, scalar quantities such as the virtual work and the kinetic and potential energies are used to develop the equations of motion of the body and in this case there is no need to study the equilibrium of the bodies in the system separately [19, 29]. Due to the linear independency of the generalized coordinates, the application of D'Alembert- lagrange's equation leads to Lagrange's Equation which is given by the equation

$$\frac{d}{dt}\left(\frac{\partial T}{\partial \dot{q}}\right) - \frac{\partial T}{\partial q} - Q = 0 \qquad 5.16$$

Where q *and* $\dot{q}$are vectors of generalized coordinate and velocities respectively. Q is the generalized force vector associated to the generalized coordinate vector [25, 29], which can be written as follow

$$Q = \begin{bmatrix} Q_{\bar{w}} \\ Q_{\theta} \end{bmatrix} \qquad 5.17$$

5.3.3 Quadratic velocity vector

By definition of the time derivative of the generalized coordinate's vector $\dot{q}$ associated to the solid body, we can find that the coordinates are the time derivative of the displacements included in the vector $\dot{\bar{w}}$ and the time derivatives of the rotation angles of the solid included in the vector $\dot{\theta}$. Starting with the translational component of the generalized coordinate vector, we get the derivative of the kinetic energy with respect to the velocity vector $\dot{\bar{w}}$ we found that

$$\frac{\partial T}{\partial \dot{\bar{w}}} = (\dot{P}^T + \dot{\bar{w}}^T A^T + \bar{w}^T \dot{A}^T\ ) M_s A \qquad 5.18$$

By finding the time derivative term for the previous equation

$$\frac{d}{dt}\left(\frac{\partial T}{\partial \dot{\bar{w}}}\right) = \ddot{\bar{w}}^T A^T M_s A + 2\dot{\bar{w}}^T \dot{A}^T M_s A + \dot{\bar{w}}^T A^T M_s \dot{A}\ + \ddot{P}^T M_s A + \dot{P}^T M_s \dot{A} + \bar{w}^T \ddot{A}^T M_s A + \bar{w}^T \dot{A}^T M_s \dot{A} \qquad 5.19$$

The same with the rotational component of the generalized coordinate vector, we can get the derivative of the kinetic energy with respect to

$$\frac{\partial T}{\partial \dot{\theta}} = (\dot{\theta}^T \bar{\bar{L}}^T + \bar{\bar{\tau}}^T) J_{\theta\theta} \bar{\bar{L}} \qquad 5.20$$

By finding the time derivative term for the previous equation

$$\frac{d}{dt}\left(\frac{\partial T}{\partial \dot{\theta}}\right) = \left(\ddot{\theta}^T \bar{\bar{L}}^T + \dot{\theta}^T \dot{\bar{\bar{L}}}^T + \dot{\bar{\bar{\tau}}}^T\right) J_{\theta\theta} \bar{\bar{L}} + \left(\dot{\theta}^T \bar{\bar{L}}^T + \bar{\bar{\tau}}^T\right) J_{\theta\theta} \dot{\bar{\bar{L}}} \qquad 5.21$$

5.3.4 Derivatives of K.E with respect to generalized coordinates

Finding the derivative of the kinetic energy of the system with respect to the displacement

$\bar{w}$ vector we found that

$$\frac{\partial T}{\partial \bar{w}} = (\dot{P}^T + \bar{w}^T \dot{A}^T + \dot{\bar{w}}^T A^T) M_s \dot{A} \quad 5.22$$

In the rotational kinetic energy equation, the term $\bar{\tau}$ represented in the solid frame of reference, it can be written in the track frame of reference using the relations defined in chapter. (3), as

$$\bar{\bar{\tau}} = B^T \bar{\tau} \quad 5.23$$

Then the kinetic rotational energy can be found by

$$T_{\theta\theta} = \frac{1}{2} \bar{\tau}^T B J_{\theta\theta} B^T \bar{\tau} + \bar{\tau}^T B J_{\theta\theta} \bar{L}\ \dot{\theta} + \frac{1}{2} \dot{\theta}^T \bar{L}^T J_{\theta\theta} \bar{L} \dot{\theta} \quad 5.24$$

The same for the rotational part, finding the derivative of the kinetic energy of the system with respect to the rotation angles vector θ, we found that the rotation angles are included only in both matrices B and $\bar{L}$ corresponding to the rotation sequence of the solid, we find that

$$\frac{\partial T}{\partial \theta_i} = \bar{\tau}^T \frac{\partial B}{\partial \theta_i} \left(J_{\theta\theta} \bar{\bar{\tau}} + J_{\theta\theta} \bar{\bar{L}} \dot{\theta} \right) + (\bar{\bar{\tau}}^T + \dot{\theta}^T \bar{\bar{L}}^T) J_{\theta\theta} \frac{\partial \bar{L}}{\partial \theta_i} \dot{\theta} \quad 5.25$$

Where

$$\theta = [\theta_i]^T ; i = x, y \text{ and } z \quad 5.26$$

5.3.5 Generalized forces associated to the generalized coordinates

The generalized forces are introduced by application of the principle of virtual work [3, 25] in both cases of static and dynamic analysis, and then the first step here is to define the virtual work for the system used

1. *Virtual Displacement*

From Eq.3.6 describing the position vector of an arbitrary point on the solid body, the virtual displacement can be written as

$$\delta r_p = A \delta \bar{w}\ + A \frac{\partial B}{\partial \theta} \bar{\bar{u}} \delta \theta \quad 5.27$$

2. *Force Vector applied on the solid*

Assuming that there is a force vector F affecting on the solid body, which represent all the forces affecting the solid, which can be friction forces, external or internal forces generated by force elements such as springs or dampers. This force vector can be written with respect to the track reference frame as

$$\bar{F} = A^T F \tag{5.28}$$

3. *Virtual work*

The virtual work produced from the application of the external force vector can be written as follow

$$\delta W = F^T A \delta \bar{w} + F^T A \frac{\partial B}{\partial \theta} \bar{\bar{u}} \delta\theta \tag{5.29}$$

Substituting from equation (5.28) in equation (5.29) we get the following equation

$$\delta W = \bar{F}^T \delta \bar{w} + \bar{F}^T \frac{\partial B}{\partial \theta} \bar{\bar{u}} \delta\theta \tag{5.30}$$

4. Generalized Force vector

Comparing this expression with the definition of the virtual work [25, 29] that can be expressed as

$$\delta W = [Q_{\bar{w}}^T \quad Q_\theta] \begin{bmatrix} \delta \bar{w} \\ \delta\theta \end{bmatrix} \tag{5.31}$$

Where $Q_{\bar{w}}$ is called the generalized force vector associated to the translational vector $\bar{w}$, and Q_θ is the generalized coordinate vector associated to the rotational angles vector θ. Furthermore the generalized forces associated to the mentioned generalized coordinates can be written as:

$$Q_{\bar{w}} = \bar{F} \tag{5.32}$$

$$Q_{\theta_x} = \bar{F}^T \frac{\partial B}{\partial \theta_x} \bar{\bar{u}} \tag{5.33}$$

$$Q_{\theta_y} = \bar{F}^T \frac{\partial B}{\partial \theta_y} \bar{\bar{u}} \tag{5.34}$$

$$Q_{\theta_z} = \bar{F}^T \frac{\partial B}{\partial \theta_z} \bar{\bar{u}} \tag{5.35}$$

5.4 Equation of motion development

5.4.1 Translational equation of motion

From Eq. 5.19 and 5.22 in Lagrange's formula we get that

$$\ddot{\bar{w}}^T A^T M_s A + 2\dot{\bar{w}}^T \dot{A}^T M_s A + \ddot{P}^T M_s A + \bar{w}^T \ddot{A}^T M_s A - Q_{\bar{w}} \tag{5.36}$$

Using the identities explained in the appendix, we replace the first and second time derivative of the track transformation matrix, also the mass matrix replaced with its value, we get that

$$m_s\ddot{\bar{w}}^T + m_s\ddot{P}^T A - 2m_s\dot{\bar{w}}^T\tilde{\bar{\tau}} + m_s\bar{w}^T\tilde{\bar{\tau}}\tilde{\bar{\tau}} - m_s\bar{w}^T\dot{\tilde{\bar{\tau}}} - Q_{\bar{w}} \qquad 5.37$$

Where the term $(\ddot{\bar{w}}^T + \ddot{P}^T A)$ represent the local acceleration of origin of the solid body seen by an observer located in the global frame of reference and it is also called the drag acceleration component, the term $(-2\dot{\bar{w}}^T\tilde{\bar{\tau}})$ represent Coriolis acceleration component, and the finally the relative acceleration component can be found in the previous equation as $\left(\bar{w}^T\,\tilde{\bar{\tau}}\tilde{\bar{\tau}} - \bar{w}^T\dot{\tilde{\bar{\tau}}}\right)$, also we can recognize both tangential component of the relative acceleration as $\left(-\bar{w}^T\dot{\tilde{\bar{\tau}}}\right)$and the normal component as $(\bar{w}^T\,\tilde{\bar{\tau}}\tilde{\bar{\tau}})$

5.4.2 Rotational Equation of motion

The same for the rotational angles vector, from Eq.5.20 and 5.25 in Lagrange's formula we get that

$$\dot{\tilde{\bar{\tau}}}^T J_{\theta\theta}\bar{\bar{L}} + \tilde{\bar{\tau}}^T J_{\theta\theta}\dot{\bar{L}} + \ddot{\theta}^T\bar{L}^T J_{\theta\theta}\bar{L} + \dot{\theta}^T\,\dot{\bar{L}}^T J_{\theta\theta}\bar{L} + \dot{\theta}^T\,\bar{L}^T J_{\theta\theta}\,\dot{\bar{L}} - \left[\frac{\partial T}{\partial\theta}\right]^T - Q_\theta = 0 \qquad 5.38$$

Where, the value of the term $\frac{\partial T}{\partial\theta_i}$ can be obtained from Eq. 5.25

5.5 Equation of motion of wheelset

The application for studying a solid moving on the track can be represented here by a wheelset system moving along the track model designed for the simulation of the movement of the general solid system defined in the previous section. The wheelset system should be defined and all the forces acting on the wheelset system including all the contact forces, moments and all applied forces like those forces produced by the force elements like dampers and springs.

5.5.1 Wheelset

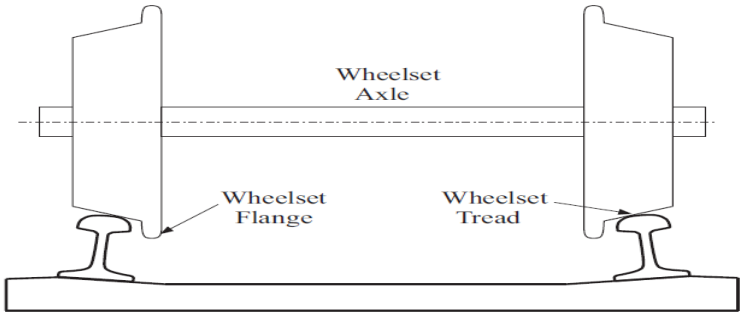

Figure 5- 2 Conventional wheelset

The fundamental component common in all conventional railway vehicles is the wheelset, it consists of two wheels rigidly fixed to a common axle [26], as shown in Fig.5.2, since the wheels are not free to rotate independently, they have the same rotational speed and a constant distance between the two wheels is mentioned. The wheels treads are conical and profiled, in order to allow them to negotiate curves without slipping. The wheelset have steering capabilities and are of the most components that affect the vehicle stability and its curving performance [9, 20]. The wheel profile is composed of two parts, the wheel tread and the wheel flange. The wheel tread is usually conned at 1/20 or 1/40 and is in contact with the rail head. The wheel flange is provided on the inside edge of the tread and, for lateral displacement, it becomes in contact with the rail edge, limiting the wheel lateral motion and reducing the probability to derailment.

5.5.2 Wheelset frame of reference

For the wheelset system represented here, it was considered to use an intermediate system of reference represented before making the final rotation about the Y- axis which is the axis of rotation of the wheelset, so the considered intermediate system of reference will be defined after two consecutive rotations about Z-axis and X-axis respectively. The importance of the use of the intermediate system of reference appeared in the definition of the contact forces and the angular velocity vectors before making the rotation of the wheelset about Y-axis to provide the simplicity of the representation of the angular velocity vector [25], which is a nonlinear function of Euler angles, in the intermediate reference frame. Fig.5.3 shows a description of the intermediate reference frame, which consists of three orthogonal coordinates $(\underline{X}\ \underline{Y}\ \underline{Z})$,where the $\underline{Z}$-axis is pointing to the vertical direction, $\underline{Y}$ -axis is parallel to the axis of rotation of the wheelset, and finally the $\underline{X}$ -axis is normal to the two other axes and pointing to the direction of motion of the wheelset.

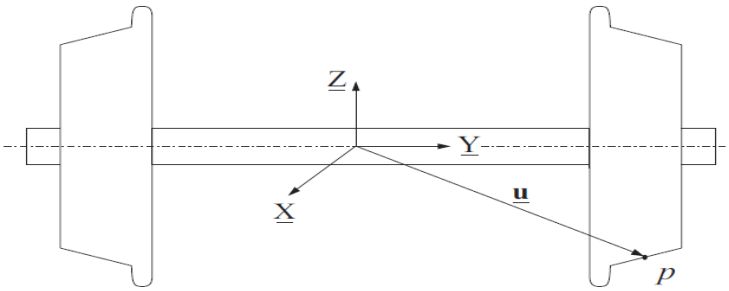

Figure 5- 3 Intermediate reference system associated to wheelset system

For an arbitrary point located on the wheel profile, the position vector be written as follow

$$\underline{u} = \left[\underline{u}_x \; \underline{u}_y \; \underline{u}_z\right]^T \qquad 5.39$$

The lower bar sign appeared in the equation means here that the quantity represented in the intermediate frame of reference. Then by defining the wheelset frame of reference in combination with the track and fixed reference frames Fig.5.4, all the kinematic and dynamic quantities calculated for the wheelset can be represented in the global reference frame as well as the track reference frames.

Contact problem for the wheel rail interaction forms a crucial part in the simulation of the MBS representing the wheelset and this problem can be divided in three distinct but correlated tasks [17]. The first is the contact geometry which is the problem of finding the location of the contact points on the profiled surfaces taking into account the relative displacements and orientation of the contact bodies, the second is the contact kinematics in which the creepages are defined at the point of contact, and finally the contact mechanics in which the contact tangential creep forces and spin moments are calculated.

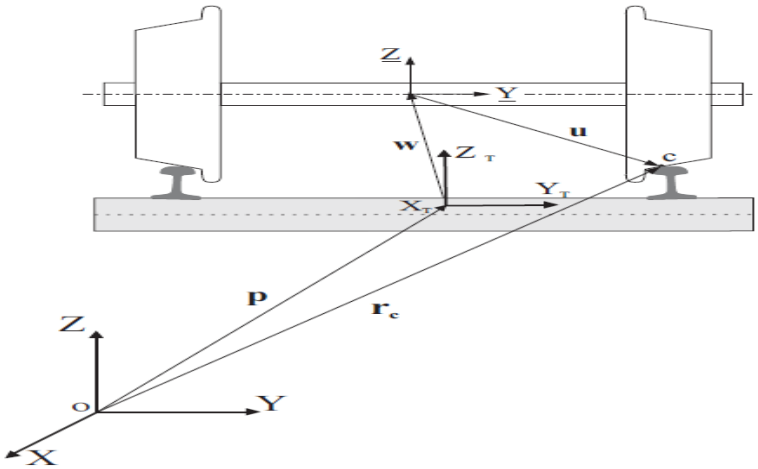

Figure 5- 4 Representation of the wheelset, track and fixed reference frame combination

5.6 Kinematic analysis of wheelset system

The kinematic analysis is done to obtain the system position and velocity vectors and determination of the generalized coordinates of the system under study. Reaching to this point, we can define the position vector of a point located on the wheelset system, the most important points in the study of the wheelset systems is the points of contact between the wheel and rail, where all the forces of contact and moments are represented. So in the following section the selected point for the analysis is the contact point located on the wheel tread as demonstrated in Fig.(5.4).

5.6.1 Position vector of the contact point

The position vector of the point of contact can be written with respect to the global reference frame as

$$r_c = P + A\bar{w} + AB_{zx}\,\underline{u}_c \qquad 5.40$$

Where B_{zx} is the intermediate transformation matrix required to transform from the intermediate to track reference frame, it is the matrix produced from two successive rotations about Z-axis and X-axis respectively, $\underline{u}_c$ is the position vector of the contact point with respect to the intermediate reference frame. By defining the overall motion of the wheelset with making the final rotation about Y-axis, the transformation from the intermediate transformation reference frame to the general solid reference frame can defined by introducing the transformation matrix By . Now all the transformation matrices are introduced between all the system of references used in the formulation of the wheelset system, and these can be explained by the Fig.5.5.

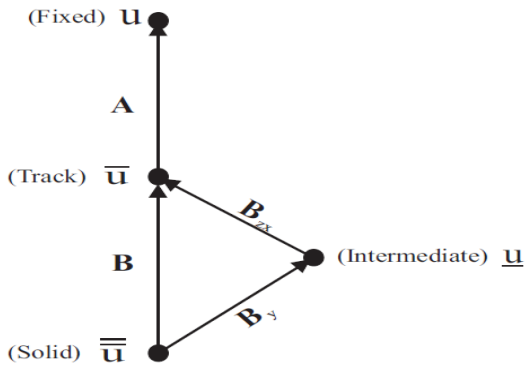

Figure 5- 5 The transformation schemes between the difference reference frames

The figure.5.5 shows that, to transform from the track reference frame to the fixed reference frame it is necessary to define the transformation matrix A, to transform from the solid reference frame to the track reference frame the matrix B is defined, the transformation from between the solid to track reference frame is achieved by two steps in which the intermediate reference system is defined. The first step is to make a transformation from solid to intermediate by defining the transformation matrix B_y

and then the second step is defined in the definition of the matrix B_{zx} required to transform from intermediate to track reference frame. Finally the position vector of the contact point can be expressed by the equation

$$r_c = P + Aw + AB\, u_c \tag{5.41}$$

Whereu_c is the local position vector of the contact point defined in the solid reference frame.

5.6.2 Velocity Vector of contact point

By making the first time derivative for the position vector Eq. 5.40, we can obtain the velocity vector of the contact point as

$$V_c = \dot{P} + \dot{A}\bar{w} + A\dot{\bar{w}} + \left(\dot{A}B + A\dot{B}\right)\bar{u}_c \tag{5.42}$$

The velocity of a point on the wheel profile consists of the summation of the total velocity of the wheelset and the circumferential velocity of the point. The total velocity of the wheelset which represent the velocity of the origin of the wheelset reference frame is equal to the velocity of the railway vehicle, it can be written as

$$V = \dot{P} + \dot{A}\bar{w} + A\dot{\bar{w}} \tag{5.43}$$

The circumferential velocity of a point on the wheel profile can be written as

$$V_{cir} = \left(\dot{A}B + A\dot{B}\right)\bar{u}_c \tag{5.44}$$

$$V_{cir} = \left(A\bar{\tau}B + A\dot{B}_{zx}B_y + AB_{zx}\dot{B}_y\right)\bar{u}_c \tag{5.45}$$

$$V_{cir} = A\bar{\tau}B_{zx}\underline{u}_c + A\dot{B}_{zx}\underline{u}_c + AB_{zx}\dot{B}_y\bar{u}_c \tag{5.46}$$

By recalling the identities used in the calculation of the time derivative of the transformation matrices A and B_{zx}, the global velocity vector of the contact point can be written as

$$V_c = \dot{P} + A\bar{\tau}\bar{w} + A\dot{\bar{w}} + A\bar{\tau}B_{zx}\underline{u}_c + A\dot{B}_{zx}\underline{u}_c + AB_{zx}\frac{\partial B_y}{\partial\theta_y}\,\dot{\theta}_y\,B_y^T\underline{u}_c \tag{5.47}$$

This can be written with respect to the intermediate reference system in the form,

$$\underline{V_c} = B_{zx}^T A^T\, V_c \tag{5.48}$$

$$= B_{zx}^T A^T\dot{P} + B_{zx}^T\bar{\tau}\bar{w} + B_{zx}^T\dot{\bar{w}} + B_{zx}^T\bar{\tau}B_{zx}\underline{u}_c + B_{zx}^T\dot{B}_{zx}\underline{u}_c + \frac{\partial B_y}{\partial\theta_y}\dot{\theta}_y B_y^T\underline{u}_c$$

5.6.3 Wheel-Rail contact forces

In the presentation of the wheel and rail models used in the formulations, both of them are considered to be a rigid body, so that the contact zone could be reduced to a contact point. In reality when two bodies are in contact, the elastic deformation of both surfaces causes the contact to be spread over a finite area, rather than to be concentrated in a point. This finite area is known as the contact patch. In railway vehicle dynamics, when a wheel rolls over the rails exists a micro-slip in the contact zone, which is called creep. This micro-slip together with the normal contact forces causes the tangential contact forces, known as creep forces [5, 6, 20]. In the wheel-rail contact problem, the dimension of the contact area is small when compared with the typical dimensions of the contacting bodies. Hence, the normal contact force developed in the contact area can be reduced to a single normal force. According to Hertz theory proposed here to study the wheel-rail contact problem, the dimension of the contact area are only dependent of the normal force, the material properties and the surface curvature of the contact bodies, being independent of the tangential forces that developed in the contact interface. The normal and tangential contact problems are decoupled and their solutions are treated sequentially.

5.6.4 Normal contact force

Generally in the wheel-rail interaction problem, if there is no penetration between the wheel and the rail, there is no contact and then the contact forces are null. The occurrence of the penetration is used as the basis to develop a procedure to evaluate the local deformation of the bodies in contact. These forces are calculated as being equivalent to those that would appear if the bodies in contact were pressed against each other by external static force [20, 24, 28]. This means that the contact forces are treated as elastic forces expressed as functions of the co-ordinates and velocities of the two bodies. The procedure proposed here for the calculation of the normal contact force depends on Hertz contact model for calculating the normal force applied at the contact point between the wheel and the rail. The direction of the normal force is determined from the normal vector to the wheel and rail surfaces at the point of contact.

5.6.4.1 Hertz's Normal contact force

Fig.5.6. shows the interaction between the rail and the wheel, and the radius of curvature of both the wheel and the rail was defined as shown in the figure below. The principle rolling radius of the wheel is R_1 , R_3 is the transversal radius of curvature of the wheel at the point of contact, R_2 is the transversal radius of curvature of the rail which usually has infinity value, and R_4 is the principal rolling radius of the rail at point of contact. The normal contact force produced at the point of contact can be calculated through the following expression.

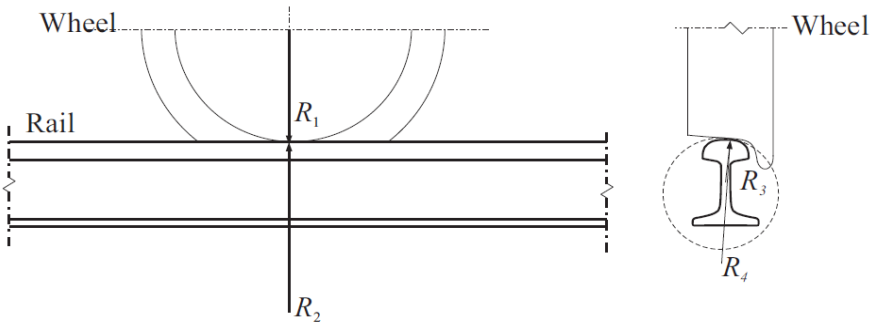

Figure 5- 6 Wheel and rail radii of curvature

$$F_z = \left(\frac{\delta^3}{r^3 \left(\frac{3}{4}(K_w + K_r)\right)^2 \left(\frac{A-B}{2}\right)} \right)^{0.5} \qquad 5.49$$

Where F_z is the normal contact force, δ is the amount of indentation or the penetration between the wheel and the rail, K_w and K_r are the material parameters of the wheel and the rail respectively, and can be calculated through the expression

$$K_w = \frac{1 - \nu_w^2}{E_w} \; ; \qquad K_r = \frac{1 - \nu_r^2}{E_r} \qquad 5.50$$

Where ν_w and ν_r are the poisson's ratio for the wheel and rail materials respectively, E_w and E_R are young's modulus of elasticity of the wheel and rail materials. The parameter in Eq. 5.49 can be found from Hertz's table 2, by interpolation between the values of the angular parameter Θ [20, 29], which can be calculated by the following expression

$$\Theta = arccos\left(\frac{A - B}{A + B}\right) \qquad 5.51$$

Where A and B are geometrical functions related to the principle and transversal radii of curvature of the wheel and the rail, which can be found by

$$A = \frac{1}{2}(K_3 + K_4) \; ; \qquad B = \frac{1}{2}(K_1 + K_2) \qquad 5.52$$

Where K is the curvature which can be calculated through the following equation

$$K = \frac{1}{R_n} \; ; n = 1, 2, 3 \; and \; 4 \qquad 5.53$$

5.6.4.2 Size and shape of the contact patch

When two elastic bodies are pressed against each other by normal force, a contact region is formed around the point contact. The shape and size of the contact patch between the two bodies are given by Hertz contact theory [6, 9, 15, 20]. In this section we will describe the necessary expressions required to calculate the size of the contact patch. According to Hertz theory and the assumptions proposed which considered to be one of the most realistic ways of analyzing of normal wheel-rail contact. In most of the railway applications the contact ellipse is a good approximation of the real contact patch, and in our simulation here it was sufficient to use Hertz theory in the analysis of the normal contact problem. The contact patch takes the shape of an ellipse shown in Fig. 5.7

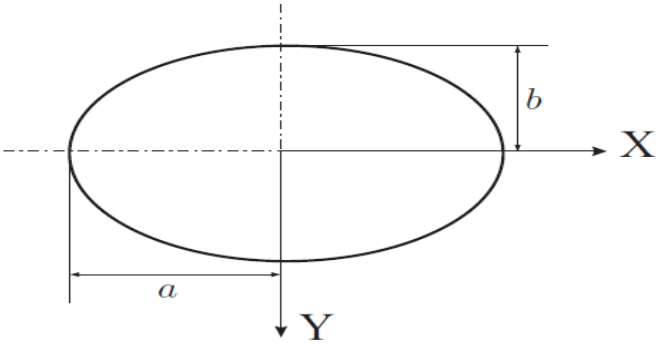

Figure 5- 7 Longitudinal and transversal semi axis of the contact ellipse

The longitudinal and transversal semi axis of the contact ellipse can be calculated by knowing the radii of curvature, the properties of the both wheel and the rail, and the normal contact force between them. The formulations used in the bibliography [5, 9], to calculate the contact ellipse semi axes can be written as

$$a = m\sqrt[3]{\frac{3}{4}F_z\left(\frac{K_w - K_r}{A + B}\right)} \qquad 5.54$$

$$b = n\sqrt[3]{\frac{3}{4}F_z\left(\frac{K_w - K_r}{A + B}\right)} \qquad 5.55$$

Where m and n are constants can be found by the interpolation between the values illustrated in Hertz table 2, for the corresponding values of the angle Θ which vary from 0 to 180^0.

5.6.5 Tangential Contact force

In the study of the wheel rail interaction phenomenon, it was found that lateral instability, hunting motion, ride quality and derailment problems are directly affected by the creep forces that occur at the contact patch. In the proceeding part, a three

dimensional rolling contact model illustrated, presenting the wheel rail interaction, to calculate the creep forces at the contact patch [20]. According to Hertz theory, an elliptical contact area was produced due to the contact between the wheel and the rail, normal stress distribution was formed. Due to the rotation of the wheel over the rail, a friction is assumed to be presented in addition to the normal stress, shear stress may occur in the contact area which result a longitudinal and lateral tangential forces. The axis of rotation of the wheel is not required to be parallel to the rail lateral axis, so a relative angular velocity about the normal axis is produced. So the contact interface tends to twist which leads to tangential stress and slip, due to the spin produced due to angular velocity at the contact area [26].

5.6.5.1 Creepage phenomena

The creep phenomenon, also known as creepages, exists when two bodies are pressed against each other with normal forces and are allowed to roll over each other. Creep may be described as a part elastic and part frictional behavior in which an elastic body, rolls over another elastic body, shares an area of contact where both slip and adhesion occur simultaneously. Therefore, a creep region of contact may be regarded as transition stat between pure rolling and pure sliding. The creepages are crucial in the calculation of the creep forces and moments that develop in the wheel rail contact region, for this purpose the accurate description of the creep phenomenon associated to the wheel-rail interaction is essential. In railway vehicle dynamics, the creep is used to characterize the relative difference in velocities between ideally rolling wheel [8, 18], having no slip in the contact, and the real one. The slip velocity between the wheel and the rail can be defined as a function of the longitudinal, lateral and spin creep which known as the creepages. For better understanding of the creep phenomenon, a wheel rolling over a rail was presented in the figure below, illustrating the longitudinal and lateral creepages as shown in Fig.5.8

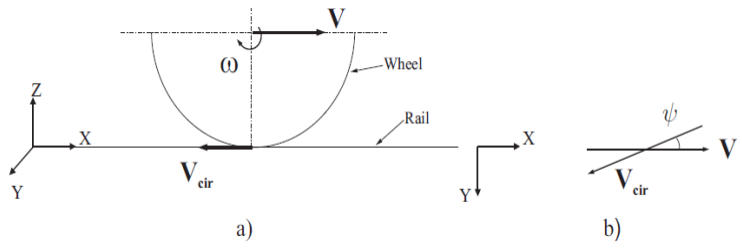

a) Longitudinal creepage b) Lateral creepage

Figure 5- 8 Wheel rolling over rail

5.6.5.2 Longitudinal Creepaage

In case of rolling without slipping, the distance traveled by the wheel in one revolution is equal to the circumference of the wheel. But when torque is applied to the wheel, the distance traveled by the wheel in the forward direction is less than the

circumference. Since the wheel profile is conned then the longitudinal creep is arises when there is a difference in the rolling radii of the two wheels of the wheelset. The longitudinal creepage can be defined as [28].

$$\xi_x = \frac{Forward\ velocity\ of\ the\ wheel - Forward\ velocity\ of\ the\ rail}{Pure\ rolling\ forward\ velocity} \qquad 5.56$$

by finding the velocity vector of the point of contact represented by Eq.5.48. The longitudinal creepage can be written as

$$\xi_x = \frac{\underline{V_c}^T \underline{l}}{V} \qquad 5.57$$

Where $\underline{V_c}$ is the velocity vector of the contact point represented in the intermediate system of reference associates with the wheelset, V is the rolling velocity [18], $\underline{l_c}$ is the principal vector in the longitudinal direction as the point of contact on the wheel profile as shown in Fig.5.9.

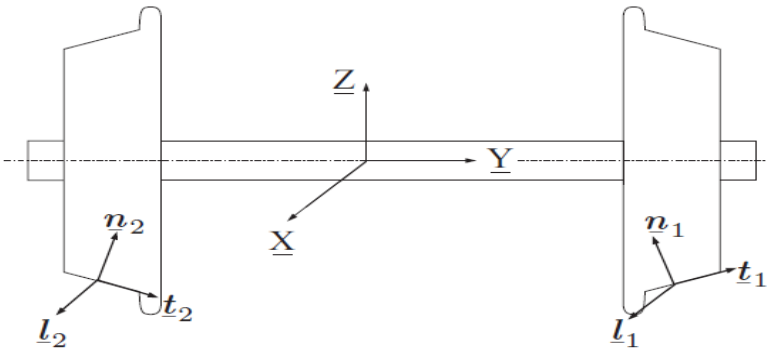

Figure 5- 9 The principal tangential, normal and longitudinal vector at the wheel contact

5.6.5.3 Lateral Creepaage

The lateral creepage ξ_y occurs when the wheelset is forced to move in a direction that makes a yaw angle ψ with respect to the rolling plane Fig.5.8, it is defined as the quotient between the lateral component of the relative velocity of the contact points, i.e. the lateral slip velocity, and the wheel forward velocity [20], lateral creepage generally can be defined as

$$\xi_y = \frac{Lateral\ velocity\ of\ the\ wheel - Lateral\ velocity\ of\ the\ rail}{Pure\ rolling\ forward\ velocity} \qquad 5.58$$

lateral creepage has a significant influence on the rails corrugations caused by the lateral creepage forces. Furthermore, the stick -slip phenomenon can be supposed to be induced between a resultant of mainly lateral and longitudinal creepage force [7].

Lateral creepage is thus likely to exist in combination with longitudinal creepage and the influence of longitudinal creepage on the mechanism of squeal noise behavior, specifically the creepage/creep force relationship, is of interest [18].to calculate the lateral creepage for the model we use here in the dynamic simulation of the wheelset system, the following expression is used

$$\xi_y = \frac{V_c^T \underline{t}}{V} \qquad 5.59$$

Where $\underline{t}$ is the longitudinal unit vector at the point of contact on the wheel profile as shown in Fig.5.8

5.6.5.4 Spin Creepage

The spin creepage is due to the component of the relative angular velocity of the two bodies normal to the contact surfaces. Generally speaking, the angular velocity of a wheel relative to the rail can be decomposed into three components; one of them is perpendicular to the contact plane, while the other two are tangent to the plane of contact [26]. However pure rolling occurred when the rolling occurs without sliding or spin [20]. The normal angular velocity is the instantaneous rate at which the wheel turns on the contact plane relative to rail, the normal component of the relative angular velocity acting through the normal direction to the contact surface represented by the unit normal vector n shown in Fig.(5.10), causes the spin (or yaw). Since the wheel profiles are coned, the rolling angular velocity of the wheel ω is not perpendicular to the vector normal to the contact area n as shown in Fig. (5.10) the consequence is that the wheel has an angular velocity ω_n relative to the rail in the contact patch.

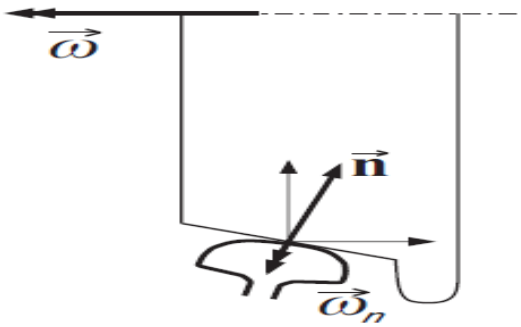

Figure 5- 10 Spin creepage

The spin creepage is given by the angular velocity of the wheel, about the normal to the contact region and can be defined by the following equation.

$$\xi_{sp} = \frac{Wheel\ angular\ velocity - Rail\ angular\ velocity}{Pure\ rolling\ forward\ velocity} \qquad 5.60$$

Which can be written in the form of

$$\xi_{sp} = \frac{\underline{\omega}^T \underline{n}}{V} \qquad 5.61$$

Where $\underline{\omega}$ the angular velocity of the wheelset is represented in the intermediate reference frame and $\underline{n}$ is the unit normal vector at the contact point.

Longitudinal and lateral creepages are dimensionless, but the spin creep has the dimension of (length^{-1}). The longitudinal creepage ξ_x is related with the difference between the rolling forward velocity and the circumferential velocity $|V - V_{cir}|$, the lateral creepage ξ_y characterize the non alignment of the wheel with respect to the rail, while the spin creepage ξ_{sp} is related with the concity of the wheel[14].

5.7 Contact forces resulting from the wheel-rail interaction

In addition to the normal contact forces acting on the contact patch, the tangential forces acting at the contact area must be determined. The creep forces and the spin creep moment result from the tangential motion of the wheel relative to the rail in the contact region, therefore they depends on the creepages. The dimension of the contact ellipse and the normal contact force calculated by Hertz formulation expressed by Eq. 5.49, are required to calculate the creep forces. The relationship between the creepages quantities, longitudinal creepage ξ_x and lateral creepage ξ_y and the spin creep moment ξ_{sp} and the creep forces can be determined by the creep force law [8, 12, 15]. Various theories was used to solve the problem of the rolling contact and calculation of the creepage forces namely, saturation of the tangential contact forces; the simplified theory of the rolling contact; linear steady state rolling contact; Heuristic nonlinear creep force model. It was proposed to use the linear steady state rolling contact to calculate the tangential contact forces at the contact patch; the name linear is directly joined to the application of Coulomb's law and the application of the conditions of Coulomb's theory for the saturation of the tangential stress. Then the linear theory is an approximation, because for large creepages, the tangential traction expressed by Coulomb's law can be violated [15, 18, 20]. For small creepages ξ_x and ξ_y and spin ξ_{sp} , the area of slip is so small that its influence can be neglected. The adhesion zone, therefore, can be assumed to cover the area of contact. Kalker's linear creep force-creepages relation [5, 8, 21, 24] are given for the longitudinal creep force as

$$F_x = -f_{33}\xi_x \qquad 5.62$$

and for the lateral creep force

$$F_y = f_{11}\xi_y - f_{12}\xi_{sp} \tag{5.63}$$

finally for the spin creep force

$$F_y = f_{11}\xi_y - f_{12}\xi_{sp} \tag{5.64}$$

The minus sign indicates that the creep force acts in the opposite direction to the creepages [15, 18], where the coefficients appeared in Eq. 5.62, 5.63 and 5.64, $f_{11};\ f_{12};\ f_{22}\ and\ f_{33}$ are Kalker's creep coefficient which can be determined by the following expressions

$$\left.\begin{array}{ll} f_{11} = Gabc_{22} & f_{12} = G\sqrt{a^3b^3}c_{23} \\ f_{22} = Ga^2b^2c_{22} & f_{33} = Gabc_{11} \end{array}\right\} \tag{5.65}$$

Then the creep force law can be written in matrix form as

$$\begin{Bmatrix} F_x \\ F_y \\ M_{sp} \end{Bmatrix} = -Gab \begin{bmatrix} c_{11} & 0 & 0 \\ 0 & c_{22} & \sqrt{ab}\,c_{23} \\ 0 & -\sqrt{ab}\,c_{23} & abc_{33} \end{bmatrix} \begin{Bmatrix} \xi_x \\ \xi_y \\ \xi_z \end{Bmatrix} \tag{5.66}$$

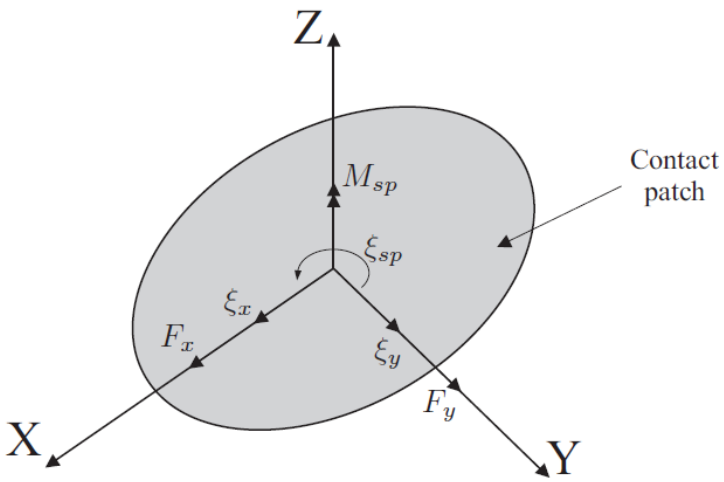

Figure 5- 11 Creepages and velocities and tangential forces on the contact patch

Where G is the combined shear modulus of the rigidity of rail and wheel materials, c_{ij} are the creepage and spin coefficients which are calculated for the exact theory can be obtained from Kalker table, and these coefficients depend on the combined poisson's ratio and the ratio between the longitudinal and transversal axis (a/b) of the contact ellipse. The coefficients c_{ij} are valid for dry friction, which, according to Kalker, corresponds to a friction coefficient of μ = 0.6. All these forces are acting in local normal and tangential coordinate directions defined by the orientation of the

contact ellipse Fig.5.11. By appropriate transformations they may be expressed as acting and counter acting forces on the wheel and the rail in their interference systems. Finally the contact loads can mainly divided into contact forces and contact moments shown in the equation of motion for the wheel set and the track [4].

5.8 Dynamic analysis of wheelset

The same as the dynamic analysis for a solid body explained in section.(5.3) we can find the equations of motion for the wheelset defined in the previous part, the only difference is the values of the generalized force associated to the wheelset generalized coordinates. For calculating the generalized force, it was supposed to use the virtual work principle [3, 25, 29] as it was explained, in the previous sections, for the calculations of the generalized forces associated to the generalized coordinates of the solid. The virtual work can be found for a wheelset system by determining the virtual displacement of a point on the wheel profile, then the calculation of the force applied at this point. Reaching to the end of the determination of the contact forces and moments at the contact patch resulting from wheel-rail interaction, also the force applied to the wheelset system due to the spring element mounted between the wheel axle and the bogie, one can find the virtual work due to these types of forces as it can be illustrated in the following sections.

5.8.1) Virtual work due to contact forces

For the contact forces applied at the contact patch, including the normal contact force, longitudinal and lateral creepage forces, with knowing the virtual displacement that can be calculated from the position vector of the contact point represented by Eq. 5.40 which can be written as

$$\delta r_c = \frac{\partial r_c}{\partial \bar{w}} \delta \bar{w} + \frac{\partial r_c}{\partial \theta} \delta\theta \qquad 5.67$$

$$\delta r_c = A\delta \bar{w} + A \frac{\partial B_{zx}}{\partial \theta} \underline{u}_c \delta\theta \qquad 5.68$$

Where

$$\frac{\partial B_{zx}}{\partial \theta} = \left[\frac{\partial B_{zx}}{\partial \theta_i}\right]^T \quad ; i = x, y \text{ and } z \qquad 5.69$$

Then the virtual work due to the contact force can be found by

$$\delta W = F_c^T \delta r_c \qquad 5.70$$

$$\delta W = F_c^T A \delta \bar{w} \; + \; F_c^T A \frac{\partial B_{zx}}{\partial \theta} \underline{u}_c \delta\theta \qquad 5.71$$

By defining the contact force vector resulting from the wheel-rail interaction and determined by Eq.5.62, Eq.5.63 and Eq.5.49 which can be written as

$$F_c = [F_x \quad F_y \quad F_z]^T \tag{5.72}$$

From Eq.4.31, the generalized forces due to the contact force can be written as

$$Q_{\bar{w}} = \bar{F}_c \tag{5.73}$$

$$Q_{\theta_x} = \underline{F_c}^T B_{zx}^T \frac{\partial B_{zx}}{\partial \theta_x} \underline{u_c} \tag{5.74}$$

$$Q_{\theta_y} = \underline{F_c}^T B_{zx}^T \frac{\partial B_{zx}}{\partial \theta_y} \underline{u_c} \tag{5.75}$$

$$Q_{\theta_z} = \underline{F_c}^T B_{zx}^T \frac{\partial B_{zx}}{\partial \theta_z} \underline{u_c} \tag{5.76}$$

Where, $\underline{F_c}$ is the contact force vector represented in the intermediate coordinate system associated to the wheelset and B_{zx} is the transformation matrix from intermediate to fixed global frame of reference.

5.8.2) Virtual work due to contact moment

The contact moment at the contact patch, produced from the spin creepage moment M_{sp}. The virtual work due to this moment M_c may be replaced by an equivalent pair of forces, f_1 and f_2, of equal magnitude and opposite directions, acting on a plane perpendicular to the direction of M_c [11] and both supposed to be acting through the longitudinal direction defined by the unit vector $\underline{l}$ and separated by the lateral unit vector $\underline{t}$, Fig. 4.12 which represent the lateral vector. If the two forces applied at the contact point can be found by:

$$\left.\begin{aligned} \underline{f_1} &= -f\underline{l} \\ \underline{f_2} &= f\underline{l} \end{aligned}\right\} \tag{5.77}$$

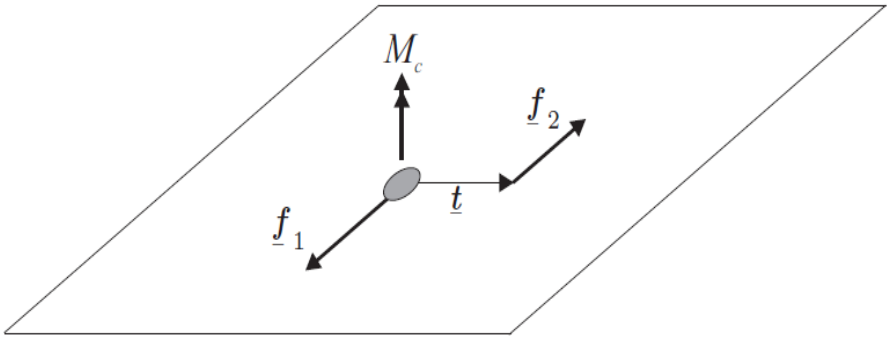

Figure 5- 12 Concentrated contact moment M_c acting on the contact area

Then the moment at the contact point can be found by

$$\underline{M_c} = \underline{t} + \underline{f_2} \tag{5.78}$$

Furthermore the virtual work due to the contact moment can be now found by the following expression

$$\delta W = \underline{f_1}\delta r_{f1} + \underline{f_2}\delta r_{f2} \tag{5.79}$$

From Eq. 5.78, we find that

$$\underline{f_2} = -M\underline{l} \tag{5.80}$$

But we know that $f_1 = -f_2$ then the virtual work due to these forces reduced to

$$\delta W = -M\underline{l}^T B_{zx}^T \frac{\partial B_{zx}}{\partial \theta} \underline{t_c}\delta\theta \tag{5.81}$$

6 Chapter Six

Case Study and Obtained Results

6.1 Introduction

In this chapter, the wheelset model used in the multibody program developed in this work was described and its dynamic behavior is studied in different operation scenarios. First the exact values for the input data required for the track pre-processing step was provided, and then the complete definition of the model used in the study is presented including all the assumptions proposed in the modeling of the wheelset.
Afterwards the construction of the multibody program implemented in MATLAB environment was described. The model performance is analyzed through the straight track stage for the time being. This chapter concludes the method and verifies the implementation of the developed multibody program which supposed to be used for the dynamic analysis of railway vehicle wheelset systems in different operation conditions.

6.2 Data Entry to the MATLAB Program

6.2.1 Track Pre-processing Stage

For the proposed track model used in this work the lengths are taken randomly, which consisting of a straight segment having a length of 1000 m, followed by a transition curve connecting the straight line stage to the plane curve stage, with a length of 200 m, then the plane curve stage which present the final stage in the designed track model having a length of 3100 m.

It was proposed to put the fixed frame of reference at which can be the position of an observer located at the starting point of the transition curve stage as it was illustrated in Fig. (6.1). For the complete definition of the track parameterization step in this part, it is necessary to define the cant angle at each track stage, for this issue defined the track height at the start and end of the track stage under study

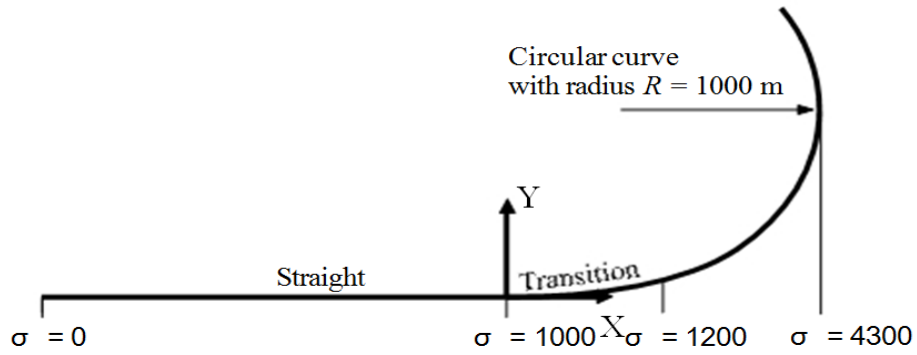

Figure 6-1 Track segments data for the designed track

The track height for the straight curve stage is defined as $h_{t,o} = 0$, and the maximum height of the track was defined as $h_{t,max} = 50 \times 10{-}3$ m , taking into account that the value of the equilibrium cant angle can be obtained from Equ.4.2

6.2.1.1 Track Model generated by MATLAB Code

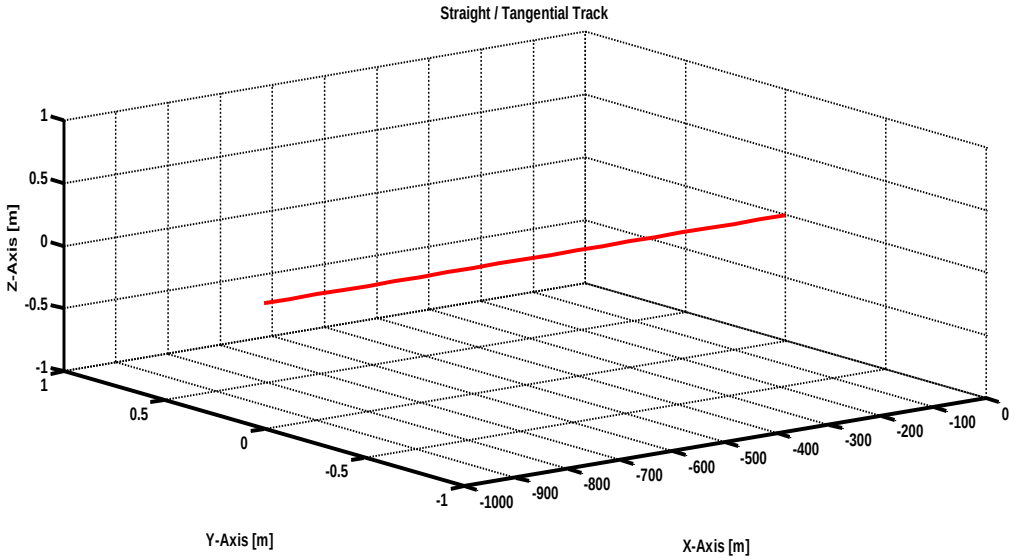

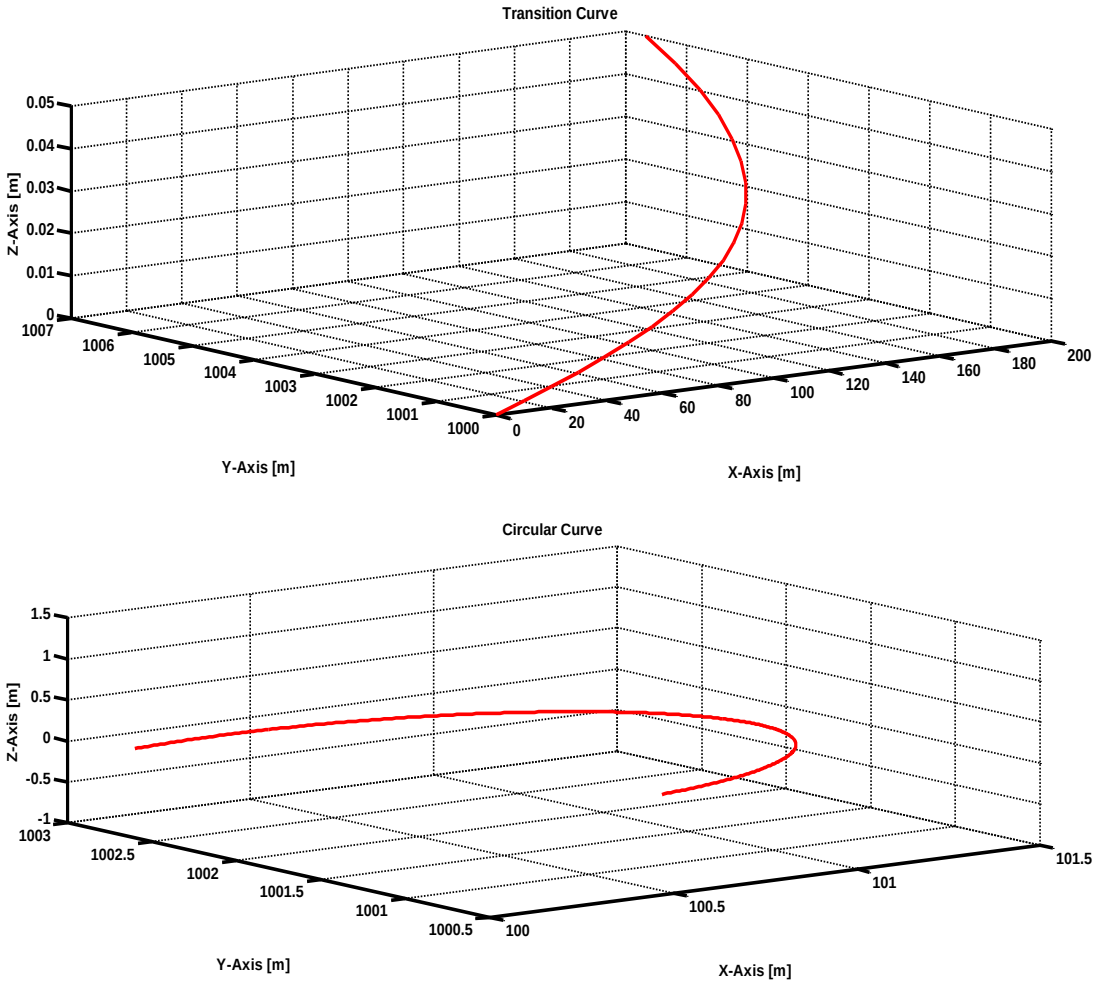

Figure 6- 2 Track model a) Straight track b) Transition track c) curved track

6.2.2 Contact Model Data entry

Since UIC60 rail profile and S1002 wheel profile is the most comment rail and wheel profile and Ethiopian Railway Corporation also use these profiles, this paper use these profiles. For each geometry used in the MATLAB, a special preprocessing function is used as to prepare the geometry.

In the pre-processing step, the contact surfaces are first entered from the measured points of the rail and wheel profile as shown below.

6.2.2.1 Wheel and rail profiles generated by MATLAB Code

In the current work a standard type of contact profile (UIC60 rail profile and S1002 wheel profile) have been used in the computation. For each geometry used in the simulation a special preprocessing function is used as to prepare the geometry used in the simulation before the program run. Fig. (6.3) and (6.4) show the profile of the wheel and rail assuming the origin of YZ axis is at the center of the two wheels or rails and assuming wheelset axle length is 1.5m.

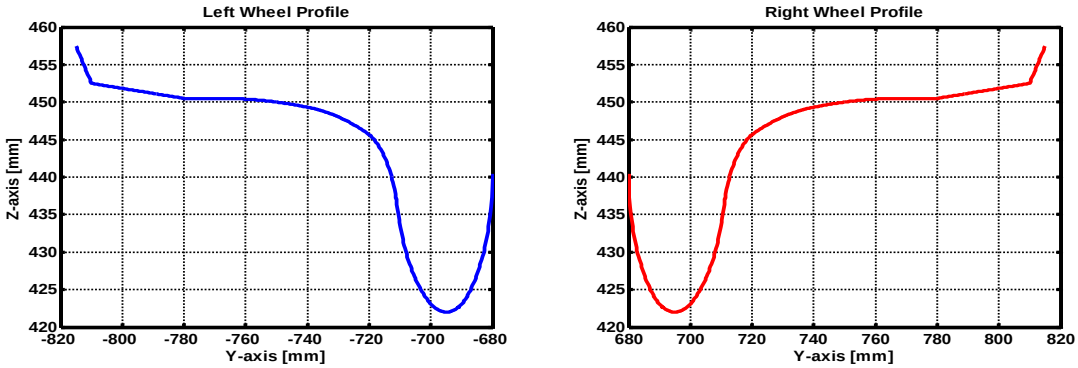

Figure 6- 3 Wheel profile

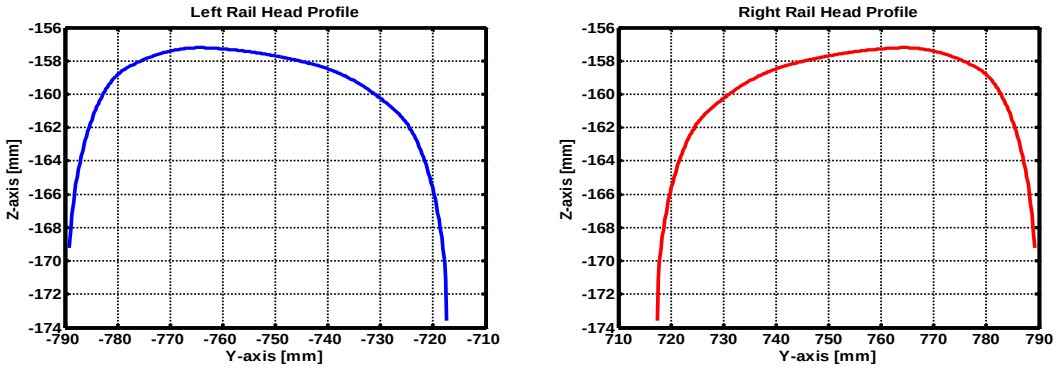

Figure 6- 4 Rail Profile

6.2.2.2 Wheel rail contact point generated by MATLAB Code

In the preprocessing step, the contact surface is first entered from the measured points of the rail and wheel as shown in Fig. (6.5). Then both profiles are brought to be in tough by putting the wheel profile just in touch with the rail profile as shown in the following figure. Assuming the origin of the YZ-axis is fixed at the center of the right wheel profile. MATLAB code is used to find the contact point of wheel profile with the rail profile for each lateral and vertical shift of wheelset on the rail provides the following figures.

For example, assuming the wheelset is fixed and the railhead is shifted from its normal position to the left with 4mm, then the right wheel-rail contact point will be y = 17.83 mm Z = 0.4914 mm

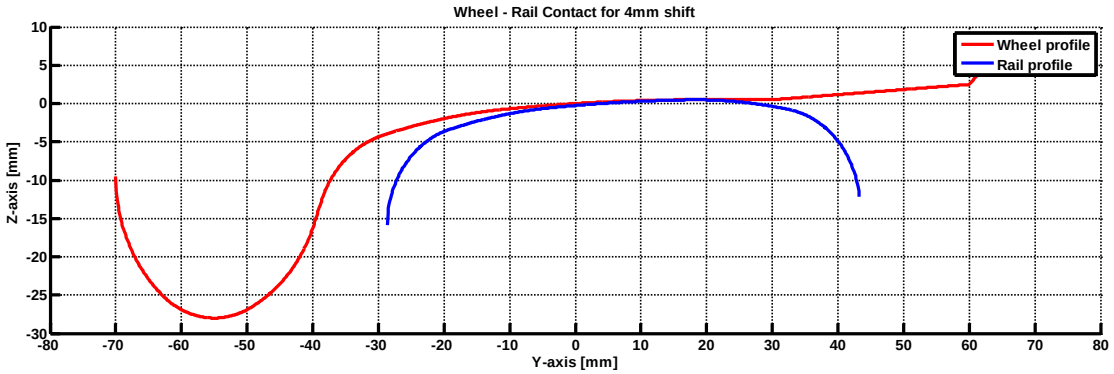

Figure 6- 5 Right Wheel-rail contact point

6.3 Multibody model of the wheelset used

According to the three-dimensional model of the wheelset proposed here, it can be shown the model has 6 DOF that means that there is no restriction made for the movement of the body in whatever direction. The system of reference of the wheelset (Xs Ys Zs) is attached to the CM of the wheelset. The position of each track frame was considered to be centered with the frame of reference of the wheelset frame of reference at a height equal to the nominal radius of the wheel profile, taking in to account the symmetry characteristics for the wheelset, then the initial position the wheelset is given by the location of its center of mass CM with respect to the corresponding track frame of reference and also with respect to the global reference frame.

The wheel set used in the model here composed of two conical wheels rigidly connected by the wheel axle. The used wheelset-rail interaction used here in the simulation is the Knife Edge model defining the shape and type of the interaction between the two surfaces of the wheel and rail profiles as it can be shown in Fig. (6.6)

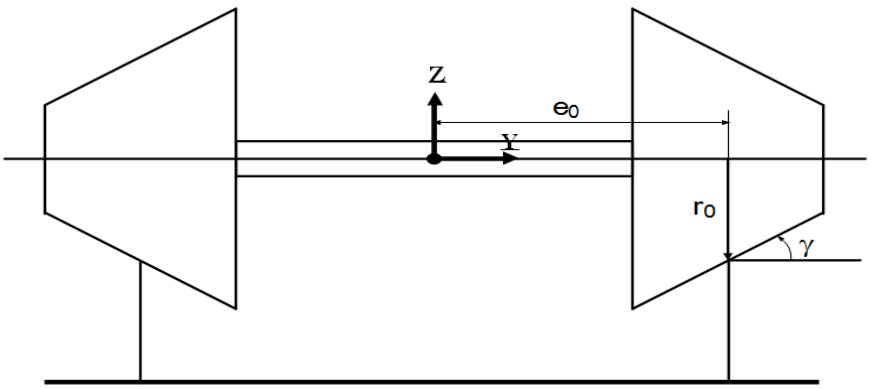

Figure 6- 6 Knife edge model of the wheel-rail interaction

To represent the contact points and determine the geometry of the contact as an important step in the contact problem, the geometric parameter and contact parameters that represent the model used here in the simulation Fig. (6.7) can be obtained from the following table

The simplified model as described in the figure having the reference frame (X Y Z) in the center of mass of the axle and the shown parameters shown on the figure can be defined as follow

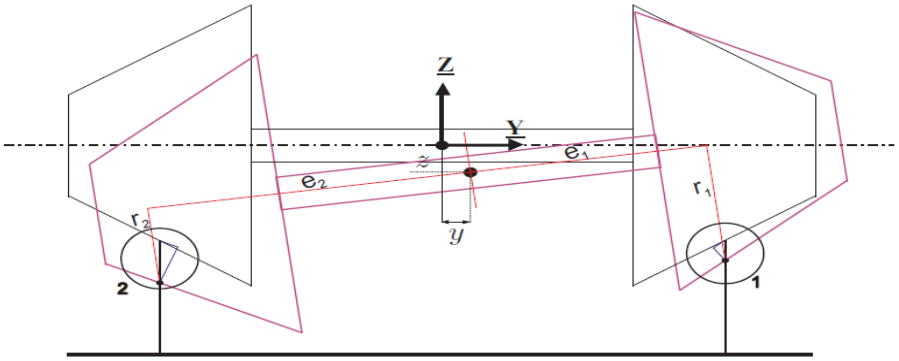

Figure 6- 7 Contact penetration produced from the movement of the wheelset

e_o: is the lateral distance from the wheelset reference associated to the center of mass of the axle frame to the nominal contact point.

- r_o : the nominal radius of rotation
- γ : the conicity angle of the wheel
- y : the lateral displacement of the wheel
- z : the lateral displacement of the wheelset
- e_1: the normal distance between the rolling radius r_1 and CM
- e_2: the normal distance between the rolling radius r_2 and CM
- r_1: the new left wheel rolling radius
- r_2: the new right wheel rolling radius
- δ: amount of approach
- ϕ: the angle of rotation about the longitudinal x-axis

After shifting the wheelset with a lateral distance y to the right the position of the center of mass of the axle is now changed and another point of contact produced due to the rotation of the axle about its center with an angle of rotation ϕ about the x-axis, producing change in the rolling radius for the left and right wheel as shown in Fig. (6.7)

Parameter	Symbol	Value	Unit
Conicity angle	γ	0.1	rad
Semi distance	e_o	0.75	m
Normal Radius	r_o	0.45	m
Poisson's ratio of the wheel	v_w	0.25	
Modulus of Elasticity of the wheel material	E_w	2.10 x 10^{11}	Pa
Poisson's ratio of the wheel	v_r	0.25	
Modulus of Elasticity of the wheel material	E_r	2.10 x 1011	Pa

Table 5.1 Geometry and contact parameter of wheelset [33]

We can now analyze the surfaces of contact after making the lateral shift with the displacement y and the rotation angle ϕ

Left Wheel

Based the geometric principle of Fig.(6.6) and (6.7), the contact geometry and amount of approach of the left wheel can be determined by the following equations

$$e_o = y + e_1 cos\phi + r_1 sin\phi \quad 6.1$$

$$r_o = z + e_1 sin\phi - r_1 cos\phi + \delta \cos(\phi + \gamma) + \tan(\phi + \gamma)\, sin(\phi + \gamma) \quad 6.2$$

$$\tan\gamma = \frac{r_1 - r_o}{e_o - e_1} \quad 6.3$$

Right Wheel

Based the geometric principle of Fig.(6.6) and (6.7), the contact geometry and amount of approach of the right wheel can be determined by the following equations

$$e_o = y - e_2 cos\phi + r_2 sin\phi \quad 6.4$$

$$r_o = z + e_2 sin\phi - r_2 cos\phi + \delta \cos(\gamma - \phi) + \tan(\gamma - \phi)\, sin(\gamma - \phi) \quad 6.5$$

$$\tan\gamma = \frac{r_o - r_2}{e_o - e_2} \quad 6.6$$

6.4 Main Structure of the Program

General Input Data

1) Common input data
   - Velocity of the train
   - Simulation time
   - Number of wheelsets
2) Input data of the track pre-processing step
   - Length of first stage (straight stage)
   - Length of second stage (Transition curve)
   - Length of third stage (Plane curve)
   - Radius of curvature of the plane curve
   - Cant h_t at the straight and plane curve stage
   - Initial position vector of the wheelset with respect to the corresponding track frame of reference
3) Input data of the wheelset
   - Wheelset mass
   - Wheelset inertia matrix
   - Wheelset parameter of the solid
   - Properties of the contact used for the contact theory
   - Geometry parameters of the wheel and rail profiles

Flow chart

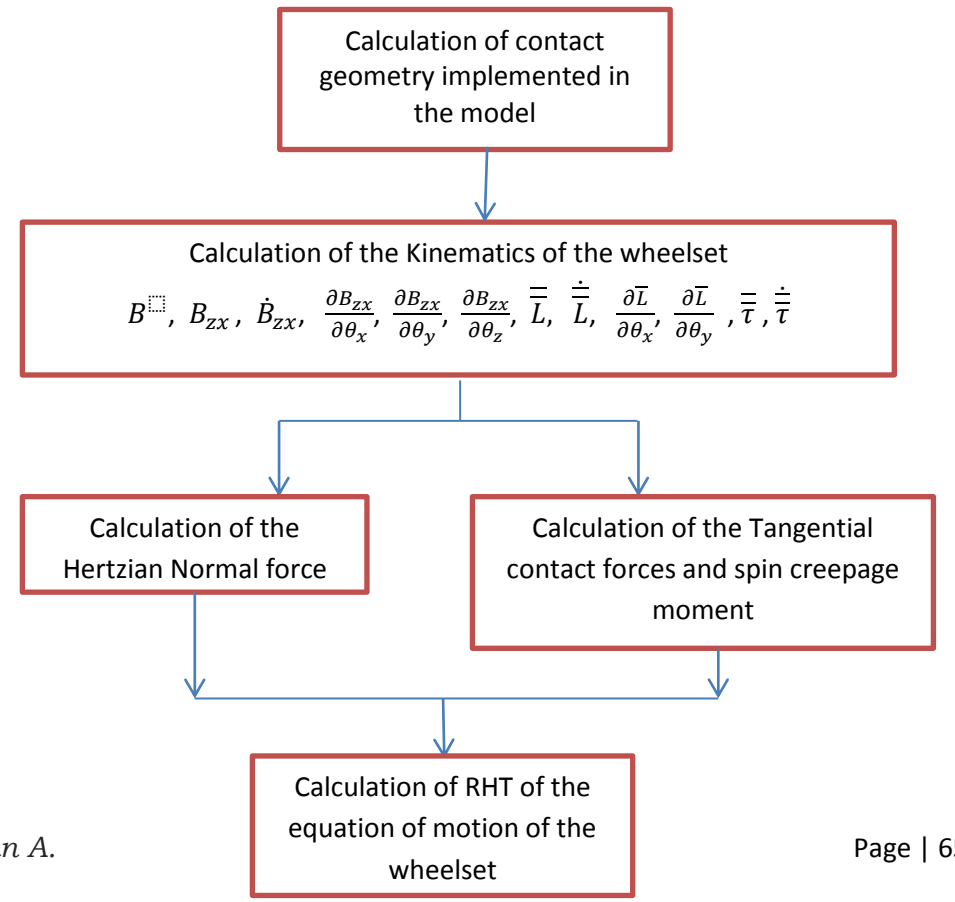

6.5 Computational Results

The simulation condition used here for the track model used in the preprocessing is defined for the simulation of a single bogie frame negotiation the straight line track and then the outcome result were compared and contrasted with one published paper (done by: D. Ramy Elsayed Shaltout, Valencia, Marzo de 2013).

In this thesis the only force considered was mass of the wheelset and the external forces from spring and damper were not considered. The contact model of the wheel-rail is a simple model of knife edge rail wheel contact.

6.5.1 Program run and extracted data

This section demonstrates the way that the dynamic analysis for the railway wheelset which is achieved by the developed computational tool including the procedure used to introduce the initial conditions before the program run. The velocity and the simulation time as well as the time step for the integration are defined starting the analysis. The extracted data from the computational tool include a vector containing the displacement and rotations of each wheelset as well as the translational and rotational velocities. As example of extracted data from MATLAB program, we can define the following output

I. Displacement
   - Lateral displacement in Y-axis

II. Rotation
   - Roll angle presenting the rotation about the X-axis
   - Pitch angle presenting the rotation about the Y-axis
   - Yaw angle presenting the rotation about the Z-axis

III. Velocities
   - The time derivative of the coordinates in the X, Y and Z direction
   - The time derivative of the rotation angle of the wheelset

IV. Normal contact force
   - Normal contact force value for the left wheel
   - normal contact force value for the right wheel

V. Creepages
   - Longitudinal creepage
   - Lateral creepage
   - Spin

VI. Tangential force
   - Longitudinal creep force
   - Lateral creep force
   - Spin creepage moment

6.5.2 Single bogie negotiating straight track

The simulation condition for the wheelset can be defined primary by description of the track geometry defined in section (5.2.1). The fixed frame of reference presenting the observer of the body is located at the point of the beginning of the transition curve.

The wheelset frame is studied at different forward velocity and for each condition the result is compared with published paper done by Mr. Ramy.

6.5.3 Stability Condition of wheelset at different forward velocities and Conicity angle

6.5.3.1 At V = 20m/s (72km/hr)

The wheelset is studied at the condition of forward velocity 20m/s which is taken randomly, a dynamic analysis is made to study the dynamic response of the wheelset moving through the straight line section. The model exhibits stable response during the motion when it is moving with a velocity of 20 m/s.

Fig (6.8 *a*) shows that the lateral displacement and yaw angle of the first wheelset of the bogie frame under study. An initial misalignment with a value of 1mm was given to the first wheelset and it is noted that the wheelset returns to its stable position after about 30 seconds.

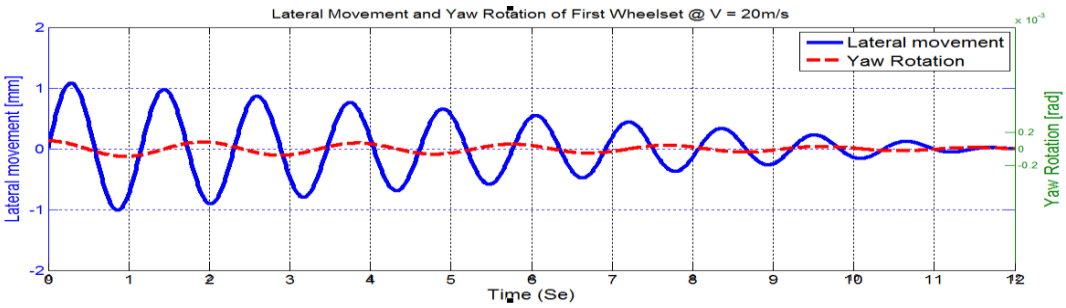

a) Found from MATLAB program

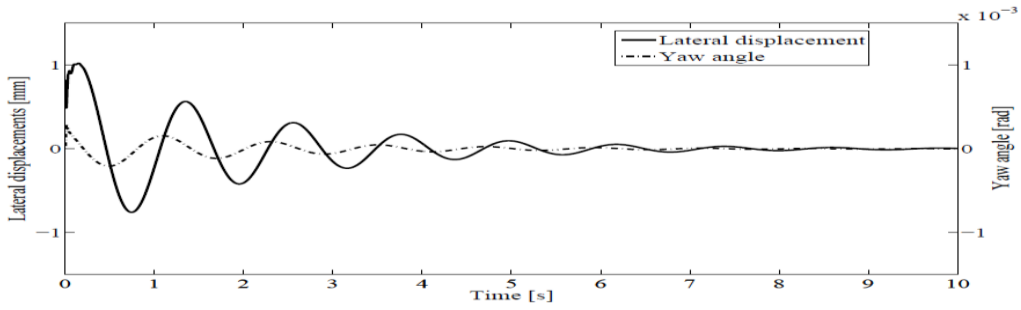

b) Copied from Mr. Ramy's paper [33] *(page 77)*

Figure 6- 8 First wheelset lateral movement and yaw rotation

Also this can be noted in Fig (6.9 *a*) representing the lateral displacement of the front and rear wheelset

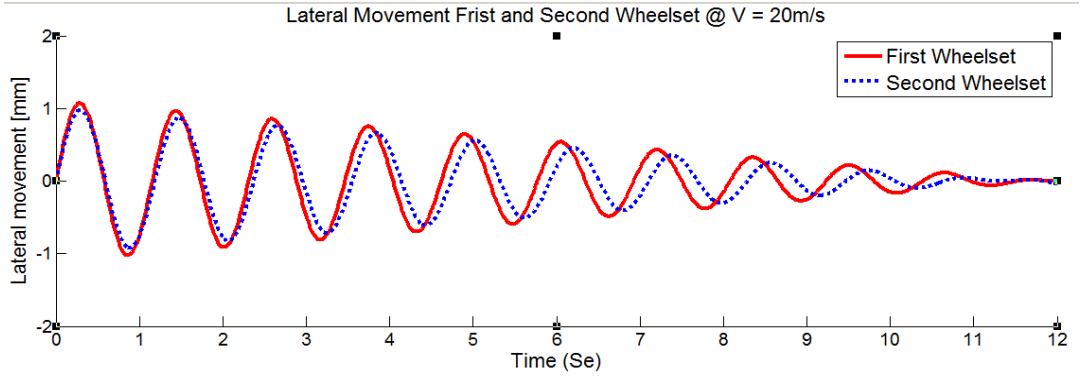

a) Found from the MATLAB program

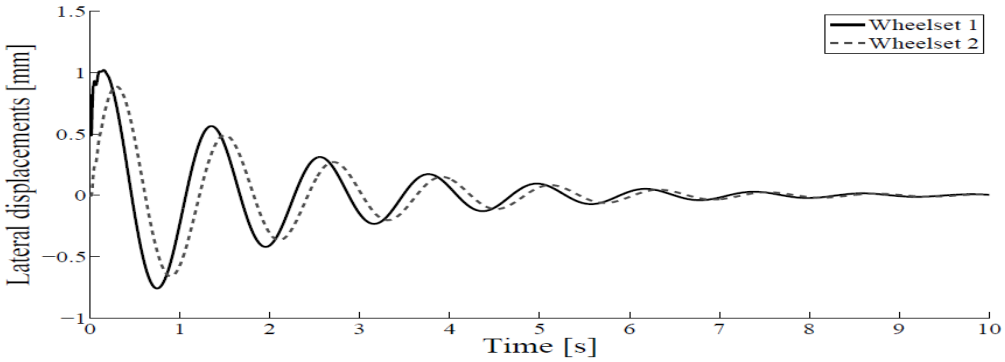

b) Copied from Mr. Ramy's paper [33] *(page 77)*

Figure 6- 9 Lateral movement of first and second wheelset at V = 20m/s

In the above two figures Fig (6.8) and Fig (6.9) we can observe that there is a difference in time taken for the wheelset to be in a stable condition, in this paper it is about 12 seconds but in Mr. Ramy's paper it is about 10 seconds. The difference comes from the condition that in my paper I didn't include the vertical and lateral forces coming from the primary and secondary suspension system but Mr. Ramy include it. The suspension systems are used to absorb the vibration and lateral movement of the wheelset and make it stable within a short period of time.

6.5.3.2 At V = 40 m/sec (144 km/hr.)

To study the instability of the system of wheelset, it was considered to increase the velocity to 40 m/sec with the same value of the initial misalignment. As noted in Fig (6.10) the lateral displacement and yaw rotation of first and second wheelset is increasing with the time and doesn't return to its stable position. This means that the system exceeds the critical velocity entering to the instability stage.

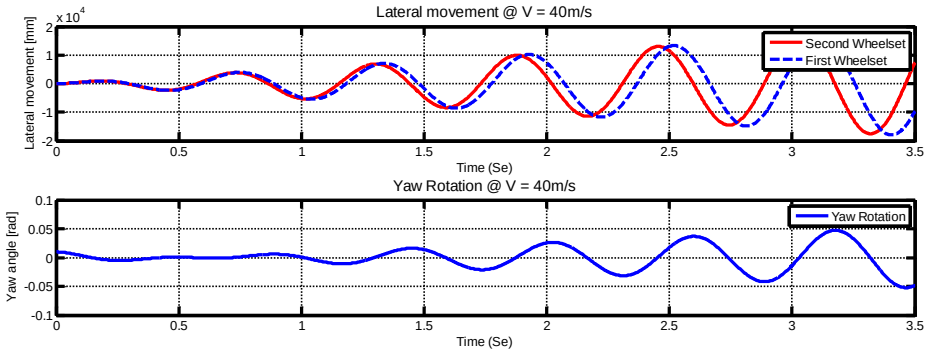

a) *Found from the above MATLAB code*

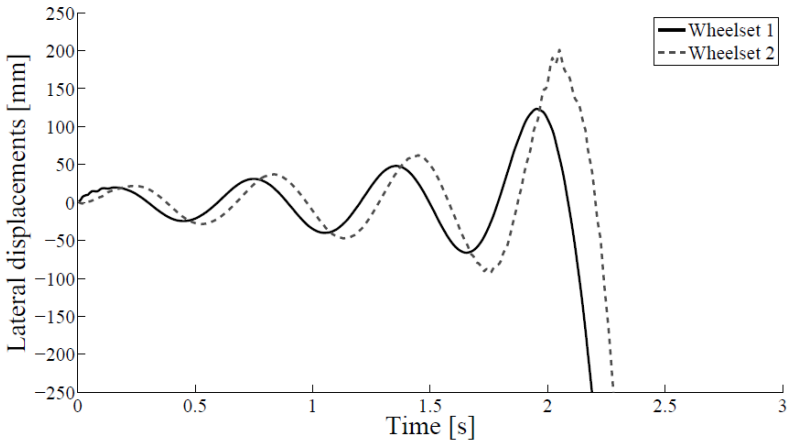

b) *Copied from Mr. Ramy's paper* [33] *(page 78)*

Figure 6- 10 Lateral movement and yaw rotation of the first and second wheelset at V = 40m/s

6.5.3.3 At V = 30m/s (108km/hr.)

At a velocity between the stability and instability velocity the wheelset oscillate with constant amplitude.

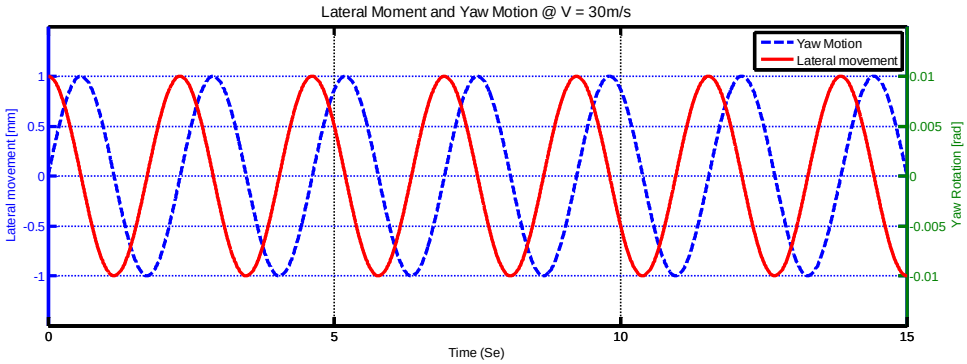

Figure 6- 11 Lateral Moment and Yaw Rotation of first wheelset at V = 30m/s

6.5.3.4 At 0 rad conicity angle (γ = 0 rad)

It is already known that, as the conicity of the wheel profile is decreased the lateral dynamics of the wheelset will also decrease and become 0 at γ = 0. But the conicity angle has an importantnce on the steering effect on curves and could not be 0. Since steering effect issue is out of the focus of this paper it is better to leave this issue by simply showing the behavior of the lateral dynamics with respect to the conicity angle.

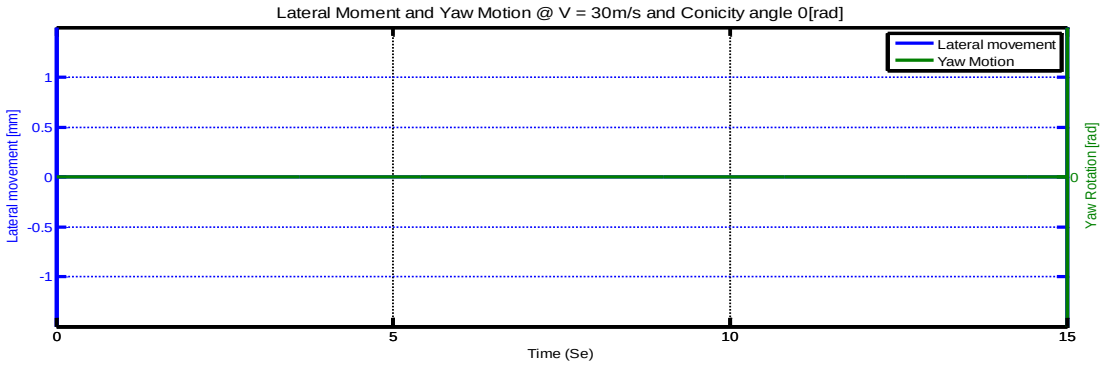

Figure 6- 12 Lateral movement and yaw rotation of the first wheelset at 0 rad conicity

In general, these MATLAB codes are used to analyze and find out the dynamic behavior of the wheelset in different conditions, which is the very important area in determining the speed of the vehicle, curvature of the track and cant angle of the track. From the above output results we can conclude that as the speed of the train increases the lateral dynamics of the wheelset is also increase and becomes unstable at above 40m/s with the above wheelset parameters.

In addition this MATLAB code is used to analyze the following parameters.

- Track geometry
- Contact profile of the wheel and rail and contact point at different lateral position for the analysis of contact area using hertz's theory
- Creepage and creep forces at the wheel- rail contact point using Kalker's theory.

7 Chapter Seven

Conclusion and Recommendation

7.1 Conclusion

In this work a computational tool used for the dynamic analysis of a wheelset system was developed using multibody formulations. This technique of multibody permit the precise analysis grand displacement between solid bodies that compose the railway vehicle systems without the models based on linearization. The computer program used for the analysis of the wheelset is developed in MATLAB environment. It was designed to be a flexible program to have the possibility to change and incorporate different contact model. The developed methodology for the analysis of railway vehicle wheelset using multibody systems formulation was studied before by other authors like A. Shaban en U. Illinois, J.L.Escalona en U.Sevilla, J. Pombo en I.S.T. Lisboa and P.Fisette U.C. Lovaina. Those authors developed other techniques based on dependent coordinates just like *Euler parameter* and *Rodriguez formula* with principal advantage which is avoiding singularity configurations. We can overcome the singularity problem as it was mentioned by the selection of the sequence of rotations applied by *Euler angles*. The selection of the intermediate reference frame associated to the wheelset systems, provides more precise definition for the contact problem. A preprocessing step was made for the track analysis to ensure the efficiency and fast calculation. A parameterization method for the track centerline was used based on the definition of the track segments analytically. A simple model for the wheel-rail contact was used in the analysis, consists of the definition of the wheels surfaces as a conical surfaces and the rails a wires and this model is known as *knife edge model*. The creepages are calculated at the wheel-rail interaction surface and the creep forces are determined using Kalker linear model. The change of the stability of the vehicle model used here was noted and it was noted that for high forward velocity, the misalignment affect the stability of the vehicle. The outcome result is compared with the already published paper of D. Ramy's [33] and there is a little difference due to the considered situation. Further enhancement will be added to the program in which the issue of the improvement of the computational efficiency and computational time cost.

Based on the outcome results of case study, It can be concluded that with a little misalignment of the wheelset center of mass will affect the lateral dynamics of the wheelset which is running at high forward velocity. The wheelset will reach its instable condition at about 40m/sec with the above wheelset parameter. The wheelset with the above given parameter and initial misalignment will have stable condition up to a forward velocity of 20m/sec. With decreasing the conicity of wheel profile lateral dynamics will also decrease as shown in Fig.(6.12) but it will have some effect on its steering system.

Using this computational tool, the behavior of wheelset lateral dynamics can be studied by iterating its parameter without producing any prototype. So this system is more effective and cost efficient due to no need of producing any prototype.

7.2 Recommendation

The development of advanced railway vehicles is a complex research field that requires new ideas and novel design solutions. So the future work in the field of railway dynamics will not finish comparing with the large challenges can be faced by the research efforts in the enhancement of passenger comfort and rapid transportation using railway transportation methods. But the future work proposed by the end of this work for the improvement of the vehicle models and enhancement methodologies, can be summarized in the following points

- Including the transition and curved tracks and track irregularities, since the computational tool (MATLAB program is developed for a straight track only)
- Including other parts of the vehicle such as body, bogie and suspension systems for the dynamic analysis of the total vehicle.
- The use of flexible multibody approach, in which the vehicle components can be modeled as flexible bodies, can be an alternative technique to be used in the future
- The use of other techniques for the calculation of the wheel-rail interaction problem, and choosing the suitable form of determination of the contact point position, including two points contact or gage contact analysis
- Including the real wheel-rail contact point model other than the knife edge contact model.
- Inclusion of vertical dynamics of the system
- The inclusion of track flexibility and track irregularity modeling of the track also seen as future goal of this work.

Reference

1) H. Akima. *A new method of interpolation and smooth curve fitting based on local procedures*. Journal of the Association for Computational Machinery, 17 (4),1970.
2) J. Ambrósio. *Advances in Computational Multibody Systems*. Springer, Dordrecht, Netherland, 2005.
3) F. M. L. Amirouche. *Fundamentals of Multibody Dynamics: Theory and Applications.* Birkhäuser, Boston, 2006.
4) C. Andersson and T. Abrahamsson. *Simulation of interaction between a train in general motion and track*. Vehicle System Dynamics, 38(6), 2002.
5) R V . Dukkipati. *Vehicle Dynamics*. CRC Press, New York, 2000.
6) V K. Grag and R V. *Dukkipati. Dynamics of Railway Vehicle Systems*. AcademicPress, New York, 1984.
7) M. Ishida, T. Moto, and M. Takikawa. *The effect of lateral creepage force on rail corrugation on low rail at sharp curves*. Journal of Wear, 253, 2002.
8) S. Iwnicki. *Simulation of wheel-rail contact forces*.
9) S. Iwnicki. *Handbook of Railway Vehicle Dynamics. CRC Press*, New York, 2006.
10) S. Iwnicki and A. H Wickens. *Validation of a matlab railway vehicle simulation using a scale roller rig*. Vehicle System Dynamics, 30, 1998.
11) J. Jalon and E. Bayo. *Kinematic and Dynamic Simulation of Multibody Systems*: The Real-Time Challenge. Springer-Verlage, New York, 1994.
12) J. J. Kalker. *Survey of wheel-rail rolling contact theory*. Vehicle System Dynamics, 8(4), 1979.
13) J. J. Kalker. *Wheel-rail rolling contact*. Journal of Wear, 144, 1979.
14) J. J. Kalker. *A fast algorithm for the simplified theory of rolling-contact*. Vehicle System Dynamics, 11(1), 1982.
15) J. J. Kalker. *Three dimensional elastic bodies in rolling contact*. Kluwer Academicpublishers, Dordrecht, 1990.
16) E. Kassa, C. Andersson, and J. C. O. Nielsen. *Simulation of dynamic interaction between train and railway turnout*. Vehicle System Dynamics, 44(3), 2006.
17) E. Meli, M. *Malvezzi*, S. Papini, L. Pugi, and A. Rindi. *A railway vehicle multibody model for real-time application*. Vehicle System Dynamics, 46(2), 2008.
18) A. D. Monk-Steel, D. J. Thompson, F. G. de Beer, and M. H. A. Janssens. *An investigation into the influence of longitudinal creepage on railway squeal noise due to lateral creepage*. Journal of Sound and Vibration, 293, 2006.
19) Parviz E. Nikravesh. *Computer-Aided Analysis of Mechanical Systems*. Parentice Hall, Engelwood cliffs, New York, 1988.
20) J. Pombo. *A multibody methodology for railway dynamics applications*. PhD thesis, Instituto Superior Técnico, Universidad Técnica de Lisboa, 2004.
21) J. Pombo and J. Ambrósio. *A computational efficient general wheel-rail contact*

detection method.

22) J. Pombo and J. Ambrósio. *Development of Roller Coaster Model*. In Proceeding of the Métodos Numéricos en Ingenier´ıa V,(J. Goicolea et al Eds.). SEMNI, Madrid, Spain, 2002.
23) J. Pombo and J. Ambrósio. *General spatial curve joint for rail guided vehicles: kinematics and dynamics*. Multibody System Dynamics, 9, 2003.
24) J. Pombo and J. Ambrósio. *A new wheel-rail contact model for railway dynamics*.Vehicle System Dynamics, 45(10), 2007.
25) A. A. Shabana. *Dynamics of Multibody Systems, Second Edition*. Cambridge University Press, Cambridge, United Kingdom, 1998.
26) A. A. Shabana and J. R. Sany. *A survey of rail vehicle track simulation and flexible multibody dynamics*. Nonlinear Dynamics, 26, 2001.
27) A. A. Shabana, K. E. Zaazaa, J. L. Escalona, and J. R. Sany. *Development of elastic force model for wheel/rail contact problems*. Journal of Sound and Vibration, 269, 2004.
28) A. A. Shabana, R. Chamorro, and C. Rathod. *A multi-body system approach for finite-element modelling of rail flexibility in railroad vehicle applications*. Proc. IMechE, Part K: Journal of Multi-body, 222(1), 2008.
29) A. A. Shabana, K. E. Zaazaa, and H. Sugiyam. *Rail Road Vehicle Dynamics* : A Computational Approach. CRC Press, Taylor and Francis group, New York,2008.
30) W. Zhai, K. Wang, and C. Cai. *Fundamentals of vehicle-track coupled dynamics.Vehicle System Dynamics*, 47(11), 2009.
31) Eva Charlotte Slivsgaard. *On the Interaction between wheels and rail in railway dynamics.* IMM – PHD 1995 -2000. Lyngby 1995
32) A.H. Wickens. *Fundamentals of Rail vehicles Dynamics.* Loughborough University, UK, 2005
33) D. Ramy Elsayed Shaltout. *Multibody approach for railway dynamics analysis.* PhD. dissertation. Valencia, 2013

Appendix A

Kinematic and Dynamic Background

A.1 Introduction

In this appendix, all the matrices used in the mathematical formulations of the models used in the kinematic presentation of the wheelset and general solid body, are presented with accurate description for all the identities and variables used in each. The calculation of each transformation matrix used in the formulation is explained in this part, its time derivative is also derived, detailed description for the inertia matrices of the solids are also included.

A.2 Rotation Matrix

A.2.1 Rotation matrix definition

In multibody systems, the components may undergo large relative translational and rotational displacements. To define the configuration of a body in the multibody system in space, one must be able to determine the location of every point on the body with respect to a selected inertial frame of reference. To this end, it is more convenient to assign for everybody in the multibody system a body reference in which the position vectors of the material points can be easily described. The position vectors of these points can then be found in other coordinate systems by defining the relative position and orientation of the body coordinate system with respect to the other coordinate systems. Six variables are sufficient for definition of the position and orientation of one coordinate system X_i Y_i Z_i with respect to another coordinate system X Y Z. As shown in Fig. A.1, three variables define the relative translational motion between the two coordinate systems. This relative translational motion can be measured by the position vector of the origin O_i of the coordinate system X_i Y_i Z_i with respect to the coordinate system X Y Z. The orientation of one coordinate system with respect to another can be defined in terms of three independent variables [25].

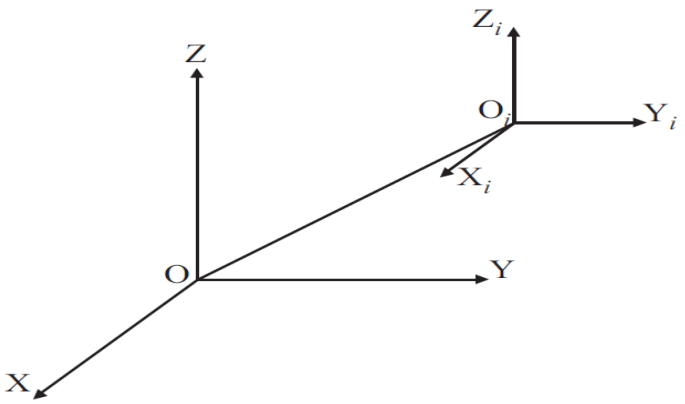

Figure A. 1 Two different coordinate systems X Y Z and X_i Y_i and Z_i

A.2.2 Derivation of the rotation matrix definition

There are several formulations used to represent the rotation matrix such as Rodriguez formula, Euler parameters and finally Euler angles formulations. These forms used to determine the rotation matrix and here we use the last method depending on the definition of Euler angles representing the required transformation

A.2.3 Euler angles

The third formulation that can be used for the representation of the rotation matrix is using Euler angles. These angles are used to carry out the transformation from one coordinate system to another using successive rotations performed in a known sequence. Furthermore these angles used to determine the successive rotations about three axes which are not orthogonal in general, so we consider the coordinate system Z,Y and X, which represent our global frame of reference and we will show the rotation matrices produced from rotation about X-axis with an angle θ_x , which can be defined in the railway application field with by the an angle φ which represent the cant angle, rotation about Y-axis with angle θ_y that can be defined in the railway application by the pitch angle θ, and finally rotation about Z-axis with an angle θz that can be defined in the railway application by the angle of attack ψ.

A.2.4 Basic Rotation

As it was introduced the orientation of a body in the space may be defined by knowing the rotations made by the body with respect to the spatial coordinates. In the following part the rotation matrices about the main spatial coordinates are represented

A.2.4.1 Rotation about X-axis

In notations used in the following context we will define the rotation matrix with the symbol A_i, where i represents the corresponding axis of rotation (i.e i = x, y, and z). The rotation matrix produced from the rotation about X-axis with an angle θ_x, Fig. A.2, can be defined as

$$A_x = \begin{bmatrix} 1 & 0 & 0 \\ 0 & cos\theta_x & -sin\theta_x \\ 0 & sin\theta_x & cos\theta_x \end{bmatrix} \qquad A.1$$

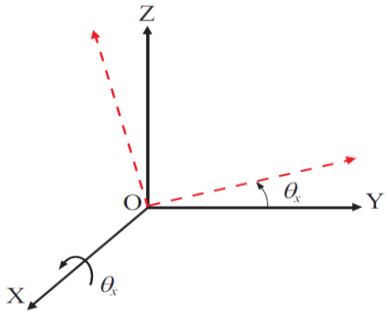

Figure A. 2 Rotation about X-axis with an angle θ_x

A.2.4.2 Rotation about Y-axis

The rotation matrix produced from the rotation about Y-axis with an angle θ_y Fig. A.3, can be defined as

$$A_y = \begin{bmatrix} cos\theta_y & 0 & sin\theta_y \\ 0 & 1 & 0 \\ -sin\theta_y & 0 & sin\theta_y \end{bmatrix} \qquad A.2$$

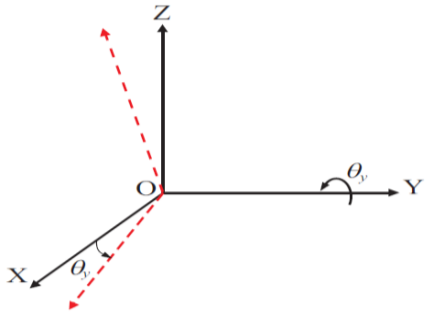

Figure A. 3 Rotation about Y-axis with an angle θ_y

A.2.4.3 Rotation about Z-axis

The rotation matrix produced from the rotation about Z-axis with an angle θz Fig.A.4, can be defined as

$$A_z = \begin{bmatrix} cos\theta_z & -sin\theta_z & 0 \\ sin\theta_z & cos\theta_z & 0 \\ 0 & 0 & 1 \end{bmatrix} \qquad A.3$$

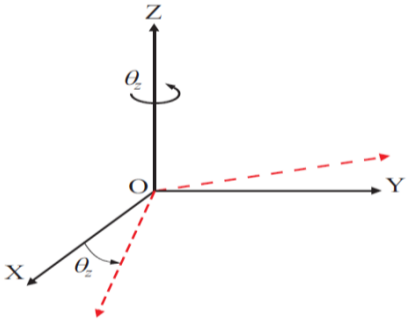

Figure A. 4 Rotation about Z-axis with an angle θ_z

A.3 Successive Rotation

In this part we will represent the final rotation matrix produced from a known sequence of successive rotations, here in this part we should have to know that there are two procedures for the representation of the successive rotations, the first called single-frame method and the other is called multi-frame method.

A.3.1 Single – Frame Method

In this method fixed frame of reference is defined and after each rotation we define the rotational axes and the unite vectors with respect to the fixed coordinate system. Now if we consider a set of consecutive rotations using the following rotation angles θ_1, θ_2...θ_n about the unite vectors v_1, v_2...v_n respectively, the rotation matrices produced after each rotation can be calculated using any formulation from the mentioned methods used to derive the rotation matrix and denoted as A1, A2... An. After n successive rotations we can calculate the final transformation matrix as

$$A = A_n A_{n-1} \dots A_2 A_1 \qquad A.4$$

where A_1 is equal to the identity matrix.

A.3.2 Multi – Frame Method

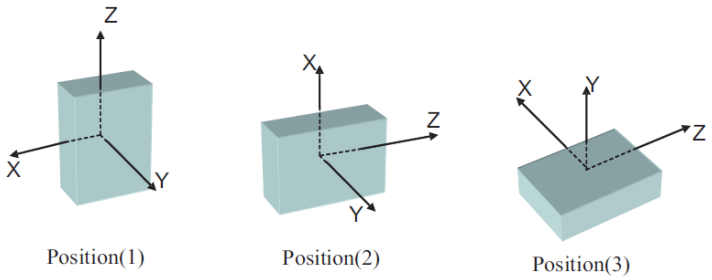

Figure A. 5 Successive rotation of the solid body about its reference coordinates

This method can be discussed by this simple example. Consider that the body shown in Fig.A.5 is subjected to two successive rotations, the first rotation is with an angle θ_1 about Y-axis producing the configuration of coordinates shown in position(2), and the second rotation with an angle θ_2 about Z-axis producing the configuration of the coordinate system shown in position(3).The orientation of coordinate system of position(2) with respect to coordinate system shown in position(1) can be described by defining the matrix A_{21}, also the orientation of the coordinate system shown in position(3) with respect to the coordinate system shown in position(2) by defining the matrix A_{32},Where n is the number of position

A.4 Successive Rotation

A.4.1 Transformation matrix definition

It is the matrix required to present the different identities such as the kinematics identities and the dynamic identities of a specified reference system with respect to another frame of reference.

A.4.2 Track transformation matrix

This matrix is the matrix required to transform from the track reference frame to the global reference frame and it is calculated here by making three consecutive rotation, first rotation about Z-axis and then about Y-axis and finally about X-axis

$$A = A_z A_y A_x \tag{A.5}$$

$$A = \begin{bmatrix} cos\theta_z cos\theta_y & -sin\theta_z cos\theta_x + cos\theta_z sin\theta_y sin\theta_x & sin\theta_z sin\theta_x + cos\theta_z sin\theta_y cos\theta_x \\ sin\theta_z cos\theta_y & cos\theta_z cos\theta_x + sin\theta_z sin\theta_y sin\theta_x & -cos\theta_z sin\theta_x + sin\theta_y sin\theta_z cos\theta_x \\ -sin\theta_y & cos\theta_y sin\theta_x & cos\theta_y cos\theta_x \end{bmatrix} \tag{A.6}$$

A.4.3 Solid transformation matrix

This matrix is the matrix required to transform from the track reference frame to the solid reference frame and it is calculated here by making three consecutive rotation, first rotation about Z-axis and then about X-axis and finally about Y- axis.

$$B = B_z B_y B_x \tag{A.7}$$

$$B = \begin{bmatrix} cos\theta_z cos\theta_y - sin\theta_z sin\theta_x sin\theta_y & -sin\theta_z cos\theta_x & cos\theta_z sin\theta_y + sin\theta_z sin\theta_x cos\theta_y \\ sin\theta_z cos\theta_y + cos\theta_z sin\theta_x sin\theta_y & cos\theta_z cos\theta_x & sin\theta_z sin\theta_y - cos\theta_z sin\theta_x cos\theta_y \\ -cos\theta_x sin\theta_y & sin\theta_x & cos\theta_x cos\theta_y \end{bmatrix} \tag{A.8}$$

A.4.4 Intermediate transformation matrix

$$B = B_z B_x \tag{A.9}$$

$$B_{zx} = \begin{bmatrix} cos\theta_z & -sin\theta_z cos\theta_x & sin\theta_z sin\theta_x \\ sin\theta_z & cos\theta_z cos\theta_x & -cos\theta_z sin\theta_x \\ 0 & sin\theta_x & cos\theta_x \end{bmatrix} \tag{A.10}$$

A.5 Angular velocity matrices

A.5.1 Absolut angular velocity matrix

$$\omega = \tau + L\dot{\theta} \tag{A.11}$$

where τ is the absolute angular velocity of the track and it can be calculated knowing the value of the angular velocity $\bar{\tau}$ represented in the track reference frame. The value of $\bar{\tau}$ can be calculated by defining the skew symmetric matrix of the track angular velocity vector represented in the track reference frame $\tilde{\bar{\tau}}$.

A.5.2 Skew symmetric matrix of the track angular velocity vector angular velocity matrix

$$\tilde{\bar{\tau}} = A^T \dot{A} \qquad A.12$$

$$\tilde{\bar{\tau}} = \begin{bmatrix} 0 & -cos\theta_y\dot{\theta}_z cos\theta_x + sin\theta_x\dot{\theta}_y & cos\theta_y\dot{\theta}_z sin\theta_x + cos\theta_x\dot{\theta}_y \\ cos\theta_y\dot{\theta}_z cos\theta_x - sin\theta_x\dot{\theta}_y & 0 & \dot{\theta}_x + sin\theta_y\dot{\theta}_z \\ -cos\theta_y\dot{\theta}_z cos\theta_x - cos\theta_x\dot{\theta}_y & \dot{\theta}_x - sin\theta_y\dot{\theta}_z & 0 \end{bmatrix} \qquad A.13$$

A.5.3 Track angular velocity vector represented in the track frame

$$\bar{\tau} = \begin{bmatrix} \dot{\theta}_x - sin\theta_y\dot{\theta}_z \\ cos\theta_y\dot{\theta}_z sin\theta_x + cos\theta_x\dot{\theta}_y \\ cos\theta_y\dot{\theta}_z cos\theta_x - sin\theta_x\dot{\theta}_y \end{bmatrix} \qquad A.14$$

A.5.4 Absolute relative angular velocity vector of the solid

The value of the matrix L depends on the rotation sequence. It represents the matrix that relates the absolute angular velocity vector of the rigid body defined in the global reference frame to the time derivative of the orientation parameters [shabana,chamarro- shabana railroad]. Then by definition of the unite vectors $v_1, v_2\ and\ v_3$ acting along the three axes of rotations Z, X, and Y respectively with respect to the global reference frame Fig.A.6, we can define the matrix $\bar{L}$ as it is represented in the track reference frame

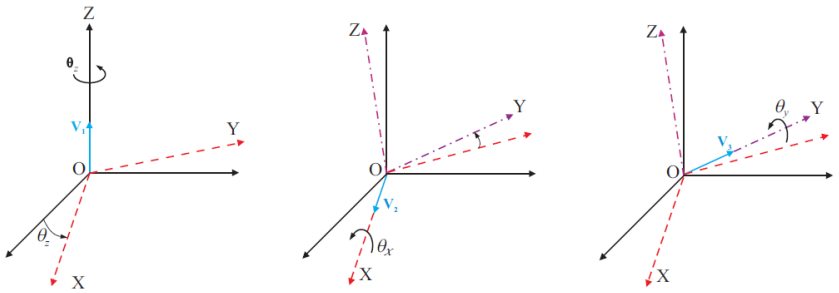

Figure A. 6 Consecutive rotation of the solid

$$v_1 = [0 \quad 0 \quad 1]^T \qquad A.15$$

$$v_2 = [cos\theta_z \quad sin\theta_z \quad 0]^T \qquad A.16$$

$$v_3 = [-sin\theta_z cos\theta_x \quad cos\theta_z cos\theta_x \quad sin\theta_x]^T \qquad A.17$$

then the relative angular velocity matrix can be defined corresponding to Fig.A.6 as follow

$$\bar{L}\dot{\theta} = [v_1 \quad v_2 \quad v_3]\dot{\theta} \qquad A.18$$

the matrix $\bar{L}$ defined in the track reference frame can be found by

$$L = \begin{bmatrix} cos\theta_z & -sin\theta_z cos\theta_x & 0 \\ sin\theta_z & cos\theta_z cos\theta_x = & 0 \\ 0 & sin\theta_x & 1 \end{bmatrix} \quad A.19$$

By knowing the transformation matrix B we can express the matrix L in the solid frame of reference as follow

$$\bar{L} = B^T L \quad A.20$$

$$\bar{\bar{L}} = \begin{bmatrix} cos\theta_y & 0 & -cos\theta_x sin\theta_y \\ 0 & 1 & sin\theta_x \\ sin\theta_y & 0 & cos\theta_x cos\theta_y \end{bmatrix} \quad A.21$$

A.6 Time derivative of transformation matrix

A.6.1 Time derivative of track transformation matrix

Recalling the expression of the transformation matrix in the track frame of reference

$$A = A_z A_y A_x \quad A.22$$

the time derivative of the matrix A can be written as

$$\dot{A} = \frac{\partial A}{\partial t} \quad A.23$$

but the matrix A is not a function of the time, then by using the chain rule , the time derivative of the matrix A can be written as

$$\dot{A} = \frac{\partial A}{\partial \theta}\frac{\partial \theta}{\partial t} \quad A.24$$

$$\dot{A} = \frac{\partial A}{\partial \theta}\dot{\theta}_z + \frac{\partial A}{\partial \theta}\dot{\theta}_y + \frac{\partial A}{\partial \theta}\dot{\theta}_x \quad A.25$$

the partial derivative of the matrix A with respect to the three rotation angles as follow

$$\frac{\partial A_x}{\partial \theta_x} = \begin{bmatrix} 0 & 0 & 0 \\ 0 & -sin\theta_x & -cos\theta_x \\ 0 & cos\theta_x & -sin\theta_x \end{bmatrix} \quad A.26$$

$$\frac{\partial A_x}{\partial \theta_x} = \begin{bmatrix} -sin\theta_y & 0 & cos\theta_y \\ 0 & 0 & 0 \\ -cos\theta_y & 0 & -sin\theta_y \end{bmatrix} \quad A.27$$

$$\frac{\partial A_x}{\partial \theta_x} = \begin{bmatrix} -sin\theta_z & -cos\theta_z & 0 \\ cos\theta_z & -sin\theta_z & 0 \\ 0 & 0 & 0 \end{bmatrix} \quad A.28$$

A.6.2 Time derivative of solid transformation matrix

The same can be done for the transformation matrix B between the solid frame of reference and the track frame of reference

$$B = B_z B_y B_x \qquad \text{A. 29}$$

$$\dot{B} = \frac{\partial B}{\partial t} \qquad \text{A. 30}$$

$$\dot{B}_{zyx} = \frac{\partial B_{zyx}}{\partial \theta_z}\dot{\theta}_z + \frac{\partial B_{zyx}}{\partial \theta_y}\dot{\theta}_y + \frac{\partial B_{zyx}}{\partial \theta_x} \qquad A. 31$$

A.6.3 Time derivative of intermediate transformation matrix

The same for the transformation matrix B_{zx}

$$B_{zx} = B_z B_x \qquad \text{A. 32}$$

$$\dot{B}_{zx} = \frac{\partial B_{zx}}{\partial t} \qquad \text{A. 33}$$

$$\dot{B}_{zx} = \frac{\partial B_{zx}}{\partial \theta_z}\dot{\theta}_z + \frac{\partial B_{zx}}{\partial \theta_x}\dot{\theta}_x \qquad A. 34$$